Light-hadron structure and dynamics in Minkowski space

Tobias Frederico
Instituto Tecnológico de Aeronáutica
São José dos Campos – Brazil
tobias@ita.br

Collaborators

Abigail Castro (ITA), E Ydrefors (IMP/Lanzhou),
JH de Alvarenga Nogueira , W de Paula (ITA),
G Salmè (INFN/Rome), D Duarte (UFSM),
JPBC de Melo (UNICSUL/UNICID)

References: PRD103, 014002 (2021); PLB820, 136494 (2021)]; PRD105 (2022) L071505; PRD 105 (2022) 114055; e-Print: 2301.11599 [hep-ph]

Physics Opportunities at an Electron-Ion Collider 2023

May 2-6, 2023 ICTP-SAIFR, São Paulo, Brazil Principia Institute

Pion - Interesting?

Pions

- Pion is the Goldstone boson associated with spontaneous symmetry breaking of chiral $SU(2)_L \times SU(2)_R$ symmetry
- Lightest hadron
- Made up of q and $\bar{q}$ constituents

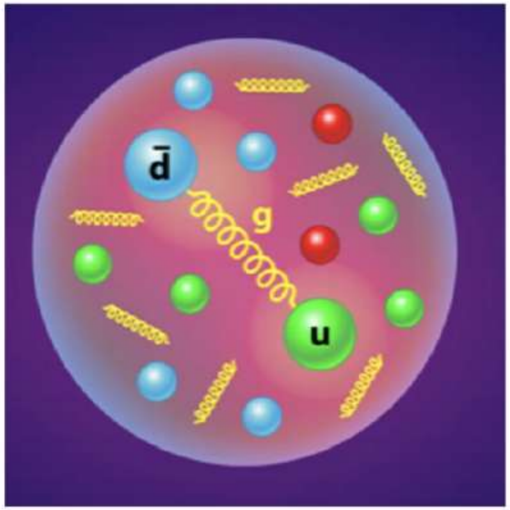

Credits to Patrick Barry

barryp@jlab.org 9

Light-front hypersurface

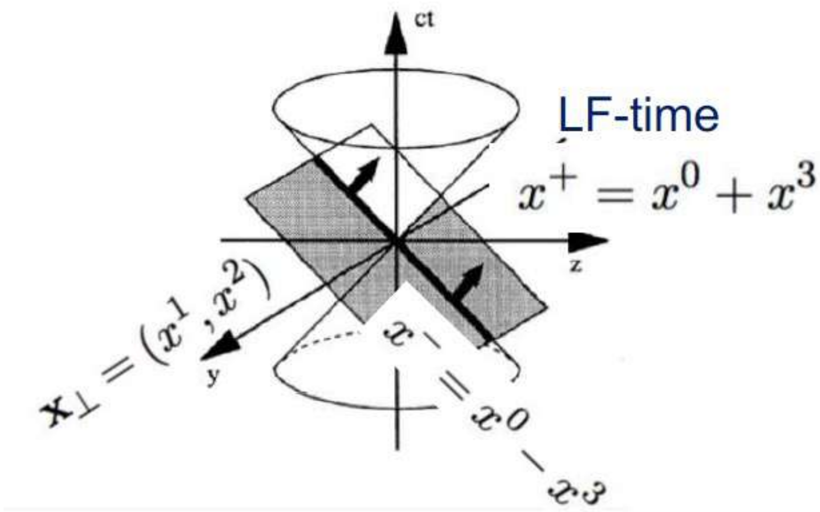

$$|\pi\rangle = |q\bar{q}\rangle + |q\bar{q}g\rangle + |q\bar{q}\,2g\rangle + \cdots$$

How to look?

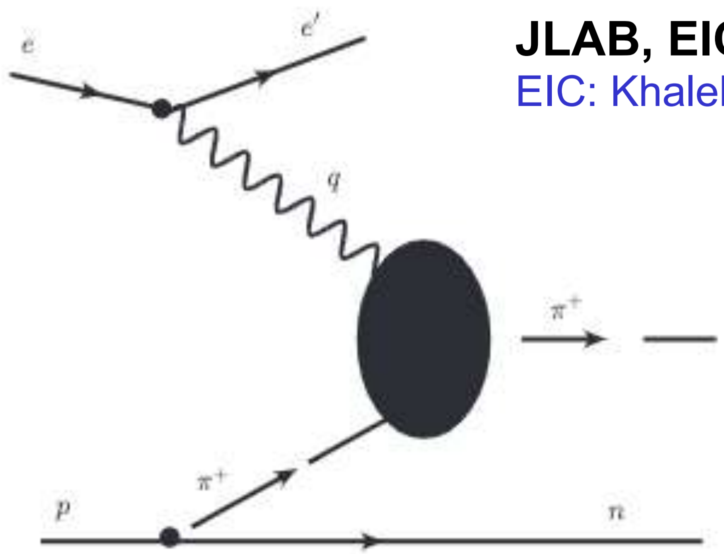

JLAB, EIC...

EIC: Khalek et al. NPA 1026 (2022) 122447

FIG. 1. Sullivan process: $ep \to e'\pi^+n$ scattering. The black blob represents the half-on-mass shell photo absorption amplitude. Diagrammatic representation of the pion pole amplitude for $p(e, e')\pi^+n$ process.

off-shell pion EM FF: Choi, TF, Ji, de Melo, PRD 100, 116020 (2019)

How to look in Detail?

Observables associated with the hadron structure

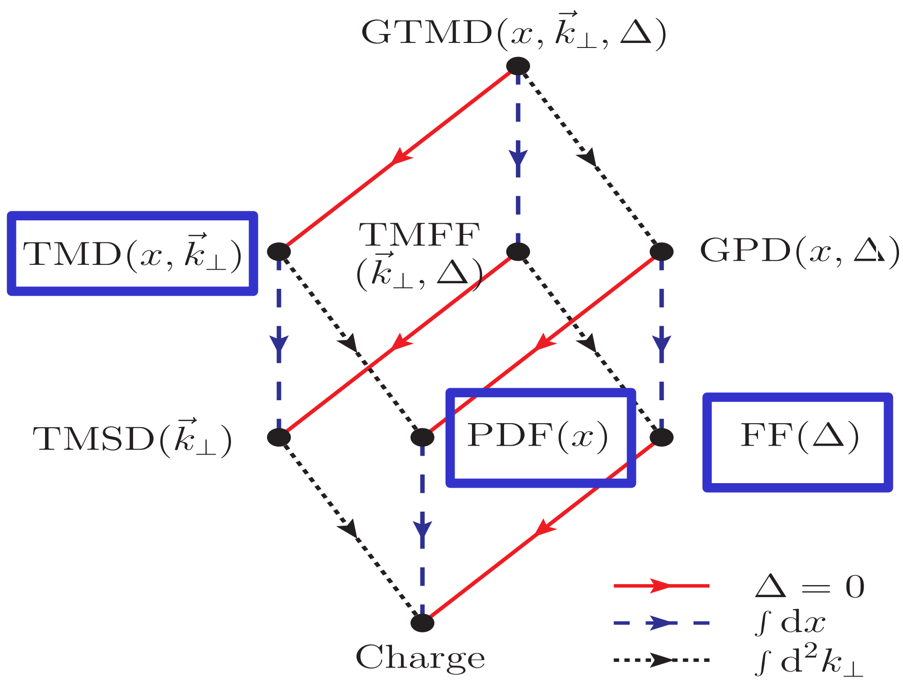

Lorcé, Pasquini, Vanderhaeghen JHEP05(2011)041

- Pion: SL form factor, PDF, TMD & 3D image

How we model:

BSE quark-antiquark & pion model

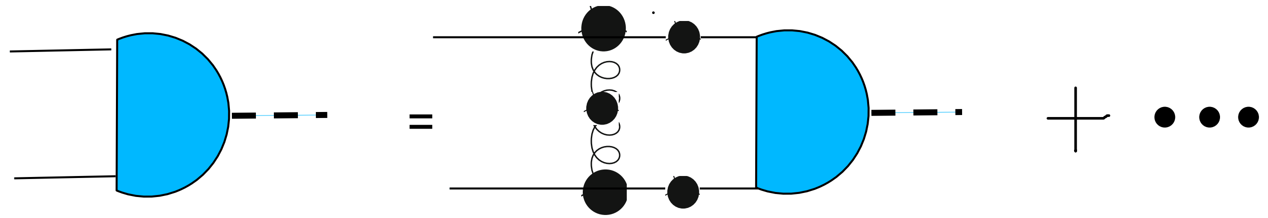

Ladder approximation (L): suppression of XL for Nc=3 in a bosonic system
[A. Nogueira, CR Ji, Ydrefors, TF, PLB777(2017) 207]

- dressed quark propagator
- dressed gluon propagator
- dressed quark-gluon vertex

- Model parameters: quark and gluon masses & quark-gluon vertex

INPUTS FROM LQCD in Landau gauge: SL momenta

Gluon propagator

$$D^{ab}_{\mu\nu}(q) = -i\,\delta^{ab}\left(g_{\mu\nu} - \frac{q_\mu q_\nu}{q^2}\right) D(q^2)$$

Dudal, Oliveira, Silva, Ann. Phys. **397**, 351 (2018)

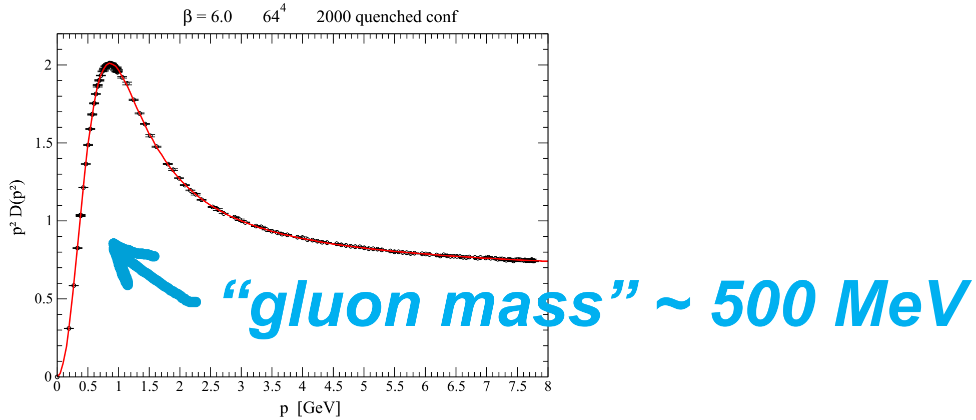

Ghost propagator

$$D_{gh}(p^2) = \frac{F(p^2)}{p^2}$$

Duarte, Oliveira, Silva, PRD 94 (2016) 014502

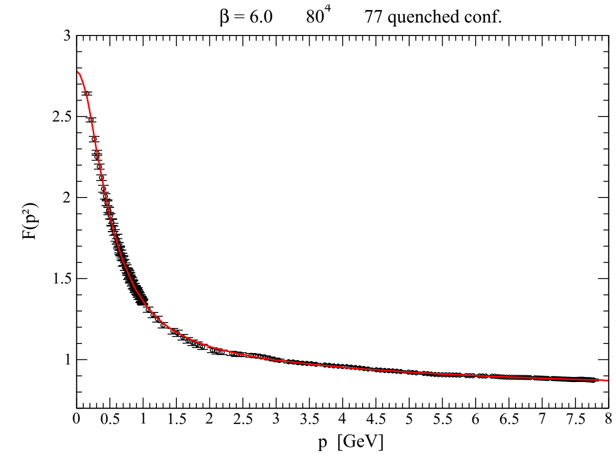

Quark propagator

Oliveira, Silva, Skullerud and Sternbeck, PRD 99 (2019) 094506

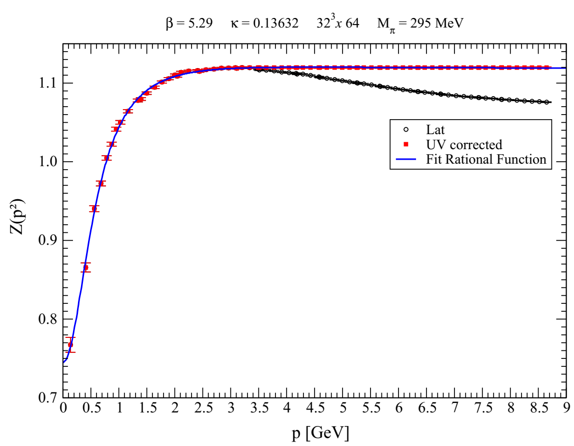

$$i\,Z(p^2)\,\frac{\not{p} + M(p^2)}{p^2 - M^2(p^2)}$$

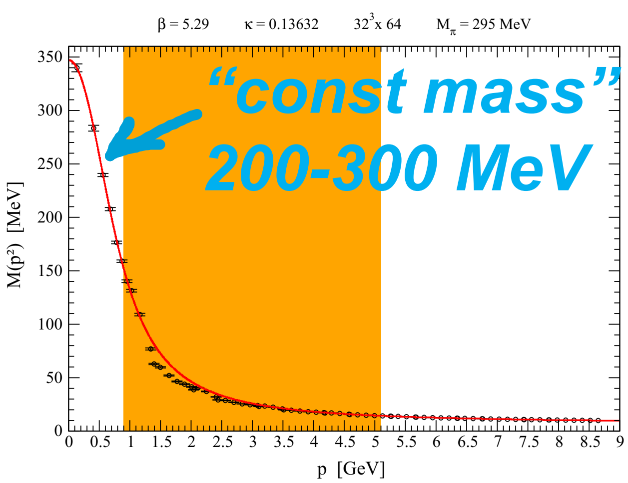

Parametrizations summarized in Oliveira, de Paula, Frederico, de Melo, EPJ C 79 (2019) 116

The Quark-Gap Equation and the Quark-Gluon Vertex

Spontaneous Chiral symmetry breaking & pion as a Goldstone boson
(origin of the nucleon mass – “constituent quarks”, Roberts, Maris, Tandy, Cloet, Maris...)

Schwinger-Dyson eq.
Quark propagator

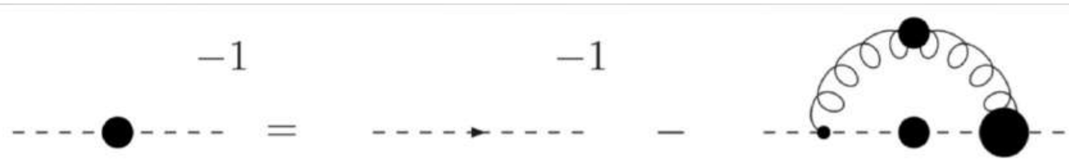

Quark-gluon vertex

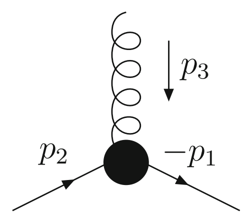

$$\Gamma^a_\mu(p_1, p_2, p_3) = g\, t^a\, \Gamma_\mu(p_1, p_2, p_3)$$

$$\Gamma_\mu(p_1, p_2, p_3) = \Gamma^{(L)}_\mu(p_1, p_2, p_3) + \Gamma^{(T)}_\mu(p_1, p_2, p_3)$$

Longitudinal component

$$\Gamma^{\mathrm{L}}_\mu(p_1,p_2,p_3) = -i\Big(\lambda_1\,\gamma_\mu \;+\; \lambda_2\,(\not p_1 - \not p_2)\,(p_1-p_2)_\mu \;+\; \lambda_3\,(p_1-p_2)_\mu \;+\; \lambda_4\,\sigma_{\mu\nu}\,(p_1-p_2)^\nu\Big)$$

Rojas, de Melo, El-Bennich, Oliveira, Frederico, JHEP 1310 (2013) 193; Oliveira, Paula, Frederico, de Melo EPJC **78**(7), 553 (2018) & EPJC 79 (2019) 116 & Oliveira, Frederico, de Paula, EPJC 80 (2020) 484

quark-gluon vertex from factors

- Schwinger-Dyson eq. quark self-energy
- Longitudinal components quark-gluon vertex
- Slanov-Taylor identity & Quark-Ghost Kernel
- Padé approximants
- Error minimization ~ 2-4%

$\alpha_s = 0.22$ and all propagators renormalised at $\mu = 4.3\,\mathrm{GeV}$

$\Lambda \sim 300$ MeV

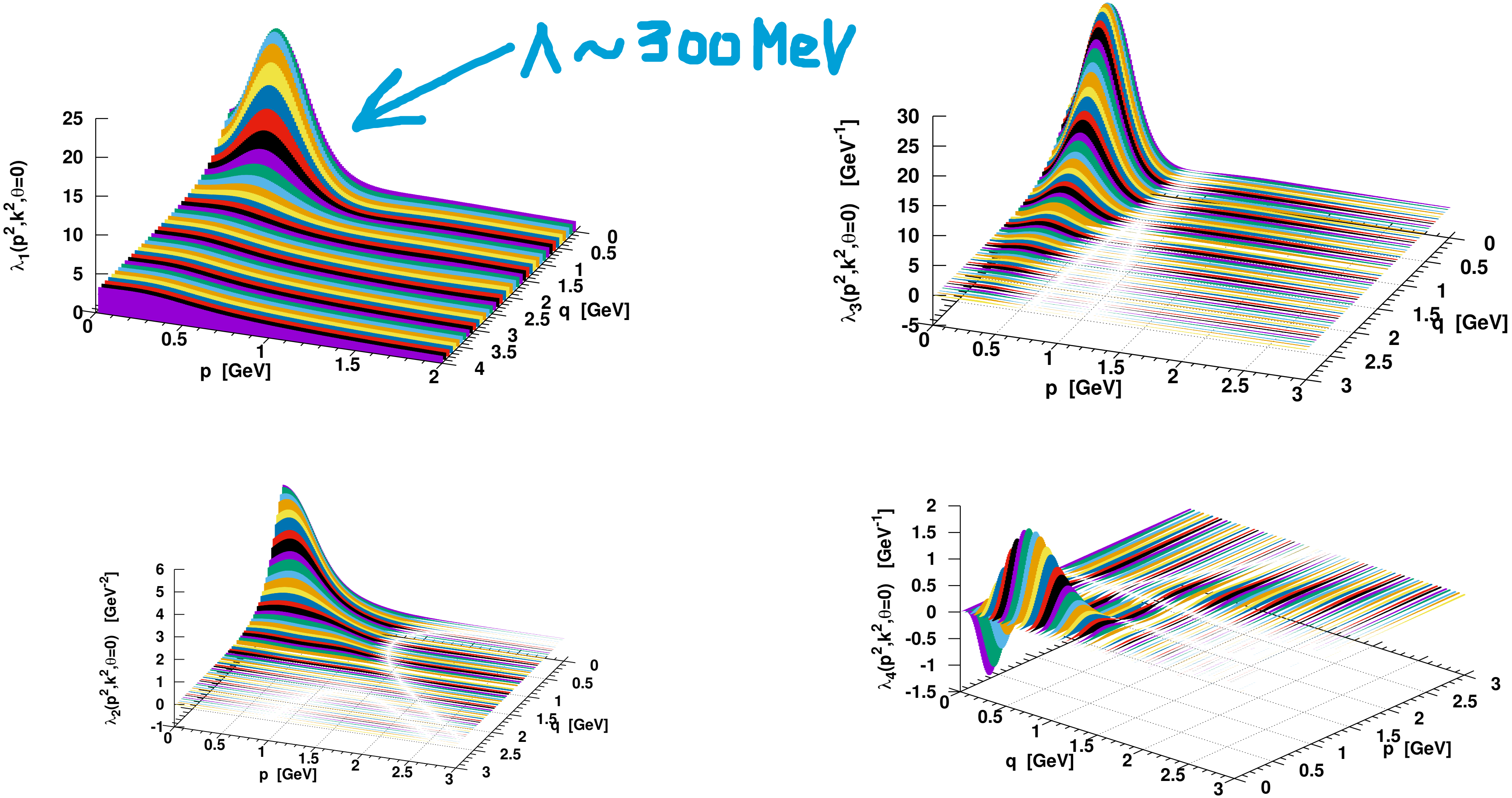

Oliveira, Frederico, de Paula, EPJC 80 (2020) 484

BSE quark-antiquark & pion model

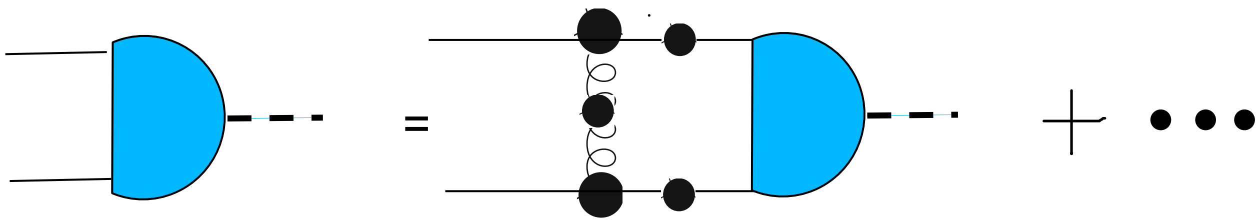

Ladder approximation (L): suppression of XL for Nc=3
[Alvarenga Nogueira, CR Ji, Ydrefors, TF, PLB777(2017) 207]

- constituent quark mass ~ 200 – 300 MeV $S(P) = \dfrac{i}{\not P - m + i\epsilon}$
- Vector exchange
  Feynman gauge
  μ ~ 500 MeV

$$iK_V^{(Ld)\mu\nu}(k,k') = -ig^2 \frac{g^{\mu\nu}}{(k-k')^2 - \mu^2 + i\epsilon}$$

- quark-gluon vertex form-factor $\lambda_1 \, \gamma_\mu$ $F(q) = \dfrac{\mu^2 - \Lambda^2}{q^2 - \Lambda^2 + i\epsilon}$
  Λ ~ 300 MeV

SOLUTION IN MINKOWSKI SPACE
[pion mass → g]

Pion BS amplitude

$$\Phi(k,p) = S_1\phi_1 + S_2\phi_2 + S_3\phi_3 + S_4\phi_4$$

$$S_1 = \gamma_5 \quad S_2 = \frac{1}{M}\not{p}\gamma_5 \quad S_3 = \frac{k\cdot p}{M^3}\not{p}\gamma_5 - \frac{1}{M}\not{k}\gamma_5 \quad S_4 = \frac{i}{M^2}\sigma_{\mu\nu}p^\mu k^\nu\gamma_5$$

Main Tool: Nakanishi Integral Representation (NIR)

(Nakanishi 1962)

Each BS amplitude component:

$$\Phi_i(k,p) = \int_{-1}^{1} dz' \int_0^\infty d\gamma' \frac{g_i(\gamma',z')}{(\gamma' + \kappa^2 - k^2 - p.kz' - i\epsilon)^3}$$

$$\kappa^2 = m^2 - \frac{M^2}{4}$$

Bosons: Kusaka and Williams, PRD 51 (1995) 7026;

Light-front projection: integration in k$^-$ Carbonell&Karmanov EPJA27(2006)1;EPJA27(2006)11;

TF, Salme, Viviani PRD89(2014) 016010,…

Fermions (0^-): Carbonell and Karmanov EPJA 46 (2010) 387;

de Paula, TF,Salmè, Viviani PRD 94 (2016) 071901;

de Paula, TF, Pimentel, Salmè, Viviani, EPJC 77 (2017) 764

Projecting BSE onto the LF hyper-plane x⁺=0

Carbonell and Karmanov EPJA 46 (2010) 387

Light-Front coordinates: $x^\mu = (x^+, x^-, \mathbf{x}_\perp)$

Within the LF framework, the valence wf is obtained by integrating the BSA on k^- (elimination of the relative LF time)

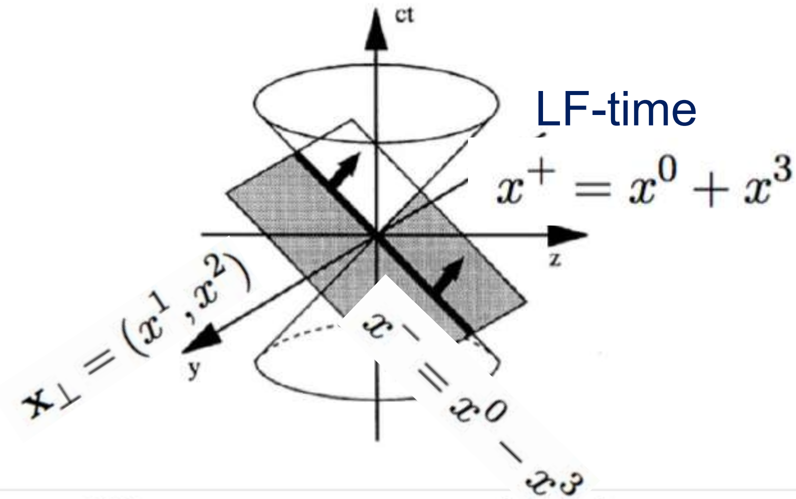

LF amplitudes $\psi_i(\gamma,\xi) = \int \frac{dk^-}{2\pi}\, \phi_i(k,p) = -\frac{i}{M}\int_0^\infty d\gamma' \frac{g_i(\gamma',z)}{[\gamma+\gamma'+m^2z^2+(1-z^2)\kappa^2]^2}$

The coupled equation system is (NIR+LF projection, Karmanov & Carbonell 2010)

$$\int_0^\infty d\gamma' \frac{g_i(\gamma',z')}{[\gamma+\gamma'+m^2z^2+(1-z^2)\kappa^2]^2} = iMg^2 \sum_j \int_0^\infty d\gamma' \int_{-1}^1 dz' \mathcal{L}_{ij}(\gamma,z;\gamma'z')g_j(\gamma,z')$$

Generalized Stietjes transform: inversible Carbonell, TF, Karmanov PLB769 (2017) 418

Kernel contains singular contributions: de Paula, TF,Salmè, Viviani PRD 94 (2016) 071901; de Paula, TF, Pimentel, Salmè, Viviani, EPJC 77 (2017) 764

The coupled equations are formally equivalent to BSE, once NIR is applied, and the validity of NIR is assessed by the existence of unique solutions to the GEVP!

BS norm, valence wave function, decay constant

Paula, Ydrefors, Alvarenga Nogueira, TF and Salme PRD 103 014002 (2021).

Normalization: $$i\,N_c \int \frac{d^4k}{(2\pi)^4}\left[\phi_1\phi_1+\phi_2\phi_2+b\phi_3\phi_3+b\phi_4\phi_4-4\;b\phi_1\phi_4-4\frac{m}{M}\phi_2\phi_1\right]=-1$$

Valence wf:
$$\left\{\begin{aligned}
\psi_{\uparrow\downarrow}(\gamma,z) &= -i\frac{M}{4p^+}\int\frac{dk^-}{2\pi}\mathrm{Tr}[\gamma^+\gamma_5\Phi(k;p)] \\
&= \psi_2(\gamma,z)+\frac{z}{2}\psi_3(\gamma,z)+\int_0^\infty\frac{d\gamma'}{M^3}\frac{\partial g_3(\gamma',z)/\partial z}{[\gamma+\gamma'+z^2m^2+(1-z^2)\kappa^2]} \\
\psi_{\uparrow\uparrow}(\gamma,z) &= \frac{\sqrt{\gamma}M}{4ip^+}\int\frac{dk^-}{2\pi}\mathrm{Tr}[\sigma^{+i}\gamma_5\Phi(k;p)] = \frac{\sqrt{\gamma}}{M}\psi_4(\gamma,z)
\end{aligned}\right.$$

$$\gamma = k_\perp^2 \text{ and } z = 2\xi-1$$

$$\psi_i\;(\gamma,z;\kappa^2)=\int_0^\infty d\gamma'\frac{g_i(\gamma',z;\kappa^2)}{[\gamma+\gamma'+m^2z^2+(1-z^2)\kappa^2]^2}$$

Generalized Stietjes transform

Carbonell, TF, Karmanov PLB769 (2017) 418

Purely relativistic nature of the aligned spin component!

Valence probability: $$P_{\rm val} = \frac{N_c}{16\,\pi^2}\int_{-1}^{1} dz \int_0^{\infty} d\gamma\ \left[|\psi^{\uparrow\downarrow}(\gamma,z)|^2 + |\psi^{\uparrow\downarrow}(\gamma,z)|^2\right]$$

Decay constant: $$f_\pi = -i\,\frac{N_c}{p^+}\int \frac{d^4k}{(2\pi)^4}\mathrm{Tr}[\,\gamma^+\gamma^5\,\Phi(p,k)] = \frac{2\,N_c}{M}\int \frac{d^2k_\perp}{(2\pi)^2}\frac{dk^+}{2\pi}\ \psi_{\uparrow\downarrow}(\gamma,z)$$

The experimental value of f_π is 130.50± 0.017 MeV

Set	m	B/m	μ/m	Λ/m	α_s $(\overline{\alpha}_s)$	P_{val}	$P_{\uparrow\downarrow}$	$P_{\uparrow\uparrow}$	f_π/m	f_π
I	187	1.25	0.15	2	5.146 (23.13)	0.64	0.55	0.09	0.414	77
II	255	1.45	1.5	1	52.78 (21.54)	0.65	0.55	0.10	0.433	112
III	215	1.35	2	1	76.28 (18.16)	0.67	0.57	0.11	0.453	98
IV	255	1.45	2	1	78.01 (18.57)	0.66	0.56	0.11	0.459	117
V	255	1.45	2.5	1	108.87 (16.87)	0.68	0.56	0.11	0.477	122
VI	255	1.45	2.5	1.1	87.66 (13.59)	0.69	0.56	0.12	0.498	127
VII	255	1.45	2.5	1.2	72.32 (11.21)	0.70	0.57	0.13	0.511	130
VIII	215	1.35	1	2	10.20 (8.50)	0.71	0.57	0.14	0.520	112
IX	187	1.25	1	2	9.96 (8.30)	0.71	0.58	0.14	0.514	96

TABLE I. Pion model with $m_\pi = 140$ MeV for different parameter sets, m and f_π in MeV. Calculated valence probability, total, antiparallel and parallel, and decay constant. The values of the coupling constant α_s and the effective strength, defined in Eq. (46), are also given.

$$\overline{\alpha}_s = \frac{\alpha_s}{\frac{\mu^2}{m^2}+0.2} \quad \text{with} \quad \alpha_s = \frac{g^2}{4\pi}(1-\mu^2/\Lambda^2)^2$$

Valence Distribution and transverse amplitudes

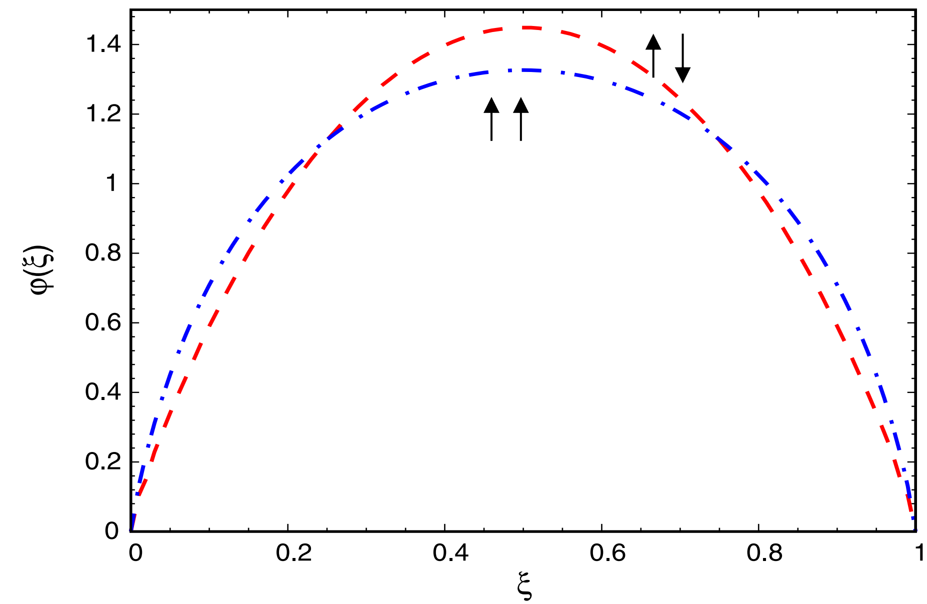

$$\varphi_{\uparrow\downarrow}(\xi) = \frac{\int_0^\infty d\gamma\, \psi_{\uparrow\downarrow}(\gamma, z)}{\int_0^1 d\xi \int_0^\infty d\gamma \psi_{\uparrow\downarrow}(\gamma, z)},$$

$$\varphi_{\uparrow\uparrow}(\xi) = \frac{\int_0^\infty d\gamma \psi_{\uparrow\uparrow}(\gamma, z)}{\int_0^1 d\xi \int_0^\infty d\gamma \psi_{\uparrow\uparrow}(\gamma, z)}.$$

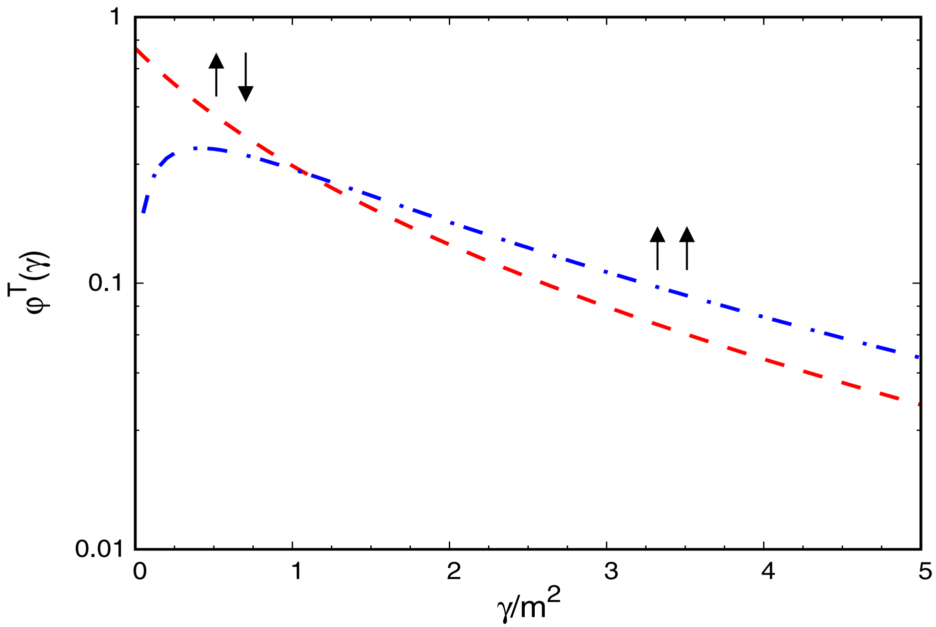

$$\varphi^T_{\uparrow\downarrow}(\gamma) = \frac{\int_0^1 d\xi\, \psi_{\uparrow\downarrow}(\gamma, z)}{\int_0^1 d\xi \int_0^\infty d\gamma\, \psi_{\uparrow\downarrow}(\gamma, z)},$$

$$\varphi^T_{\uparrow\uparrow}(\gamma) = \frac{\int_0^1 d\xi\, \psi_{\uparrow\uparrow}(\gamma, z)}{\int_0^1 d\xi \int_0^\infty d\gamma\, \psi_{\uparrow\uparrow}(\gamma, z)},$$

Valence TMD

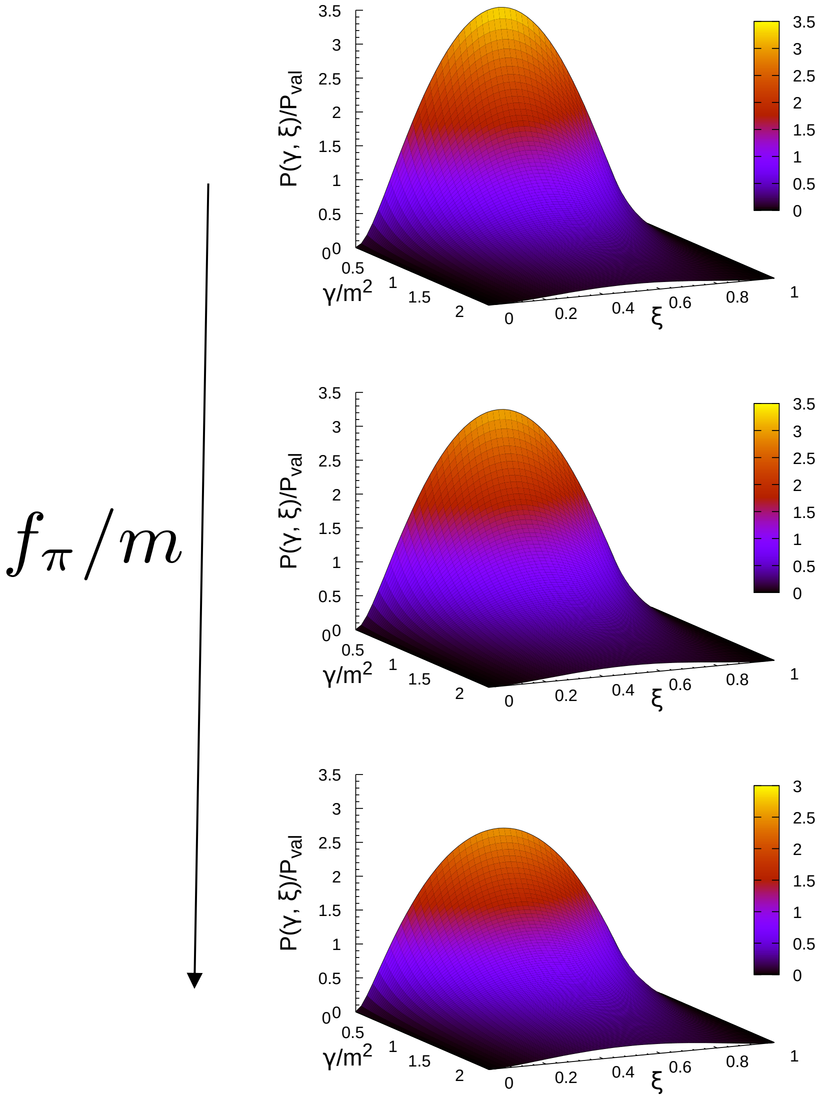

FIG. 3. 3D-valence momentum distribution as a function of ξ and $\gamma = k_\perp^2$. Panels from top to bottom represent the results for the parameter sets (II), (IV) and (VII), respectively.

$$P_{\rm val} = \int_{-1}^{1} dz \int_{0}^{\infty} d\gamma \, \mathcal{P}_{val}(\gamma, z)$$

Set	f_π/m	$\eta_{\uparrow\downarrow}$	$\eta_{\uparrow\uparrow}$	η
II	0.433	1.71	1.50	1.66
IV	0.477	1.61	1.42	1.57
VII	0.511	1.44	1.26	1.40

TABLE II. Exponent of the fit function $(1-\xi)^\eta$ $(\xi \to 1)$ for the antiparallel, parallel and total valence distributions.

3D Pion image on the null-plane

The probability distribution of the quarks inside the pion, on the light-front, is evaluated in the space given by the Cartesian product of the Ioffe-time and the plane spanned by the transverse coordinates.

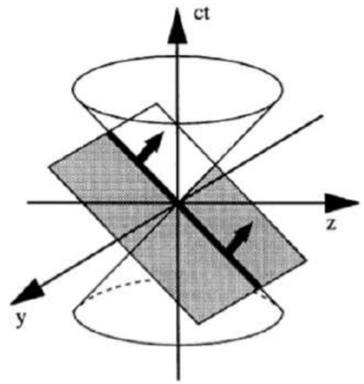

Our goal is to use the configuration space in order to have a more detailed information of the space-time structure of the hadrons.

The Ioffe-time is useful for studying the relative importance of short and long light-like distances. It is defined as:

$$\tilde{z} = x \cdot P_{target} = x^- P^+_{target}/2 \quad \text{on the hyperplane } \mathrm{x}^+ = 0$$

Miller & Brodsky, PRC 102, 022201 (2020)

$$\{\xi = k^+/p^+, \mathbf{k}_\perp\} \xrightarrow{\text{F.T.}} \{\tilde{z} = p^+x^-/2, \mathbf{b}\}$$

Ioffe-time

Phys. Lett. B **30**, 123 (1969).

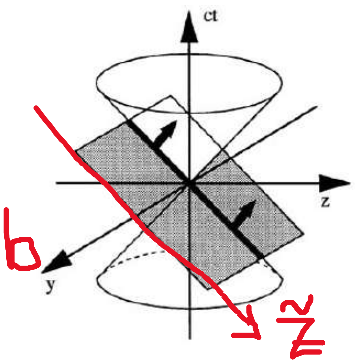

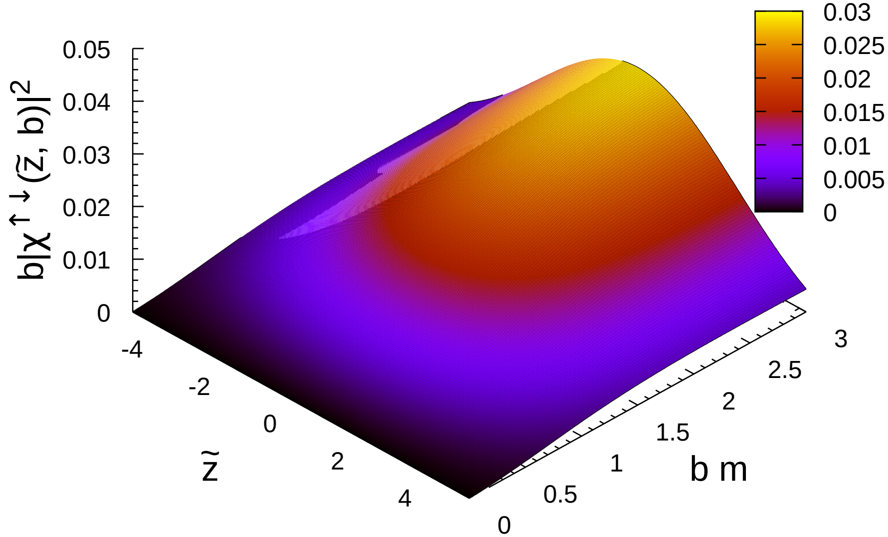

$$\tilde{\psi}_{\uparrow\downarrow}(\tilde{z}, b) = \mathrm{e}^{-b\,\kappa}\mathrm{e}^{-\frac{i}{2}\,\tilde{z}}\chi_{\uparrow\downarrow}(\tilde{z}, b)$$

$$\tilde{\psi}_{\uparrow\uparrow}(\tilde{z}, b) = \mathrm{e}^{-b\,\kappa}\mathrm{e}^{-\frac{i}{2}\,\tilde{z}}\chi_{\uparrow\uparrow}(\tilde{z}, b)$$

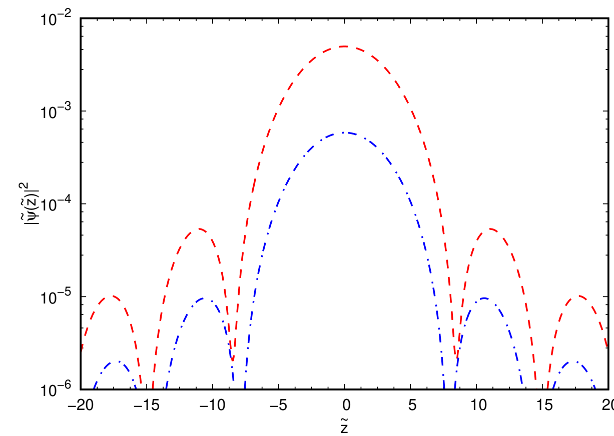

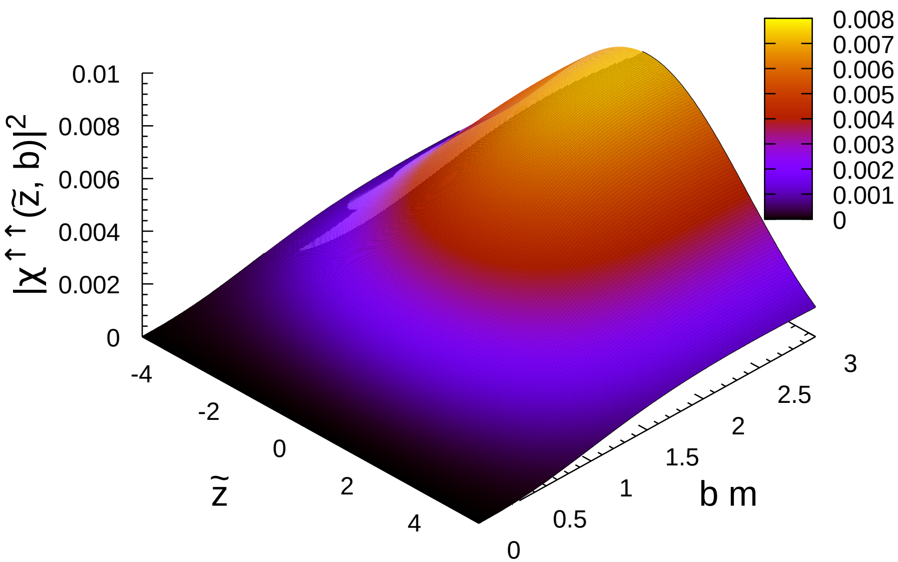

FIG. 9. Integrated probability density for the two spin components as a function of the rescaled longitudinal momentum. Dashed line: $\tilde{\psi}_{\uparrow\downarrow}(\tilde{z}) = \int_0^\infty db\tilde{\psi}_{\uparrow\downarrow}(\tilde{z}, b)$ and dash-dotted line: $\tilde{\psi}_{\uparrow\uparrow}(\tilde{z}) = \int_0^\infty db\tilde{\psi}_{\uparrow\uparrow}(\tilde{z}, b)$.

3D Pion image on the null-plane: Spin configurations

Space-time structure of the pion in terms of $\tilde{z} = x^- p^+ / 2$ and transverse coord. $\{b_x, b_y\}$

Anti-aligned

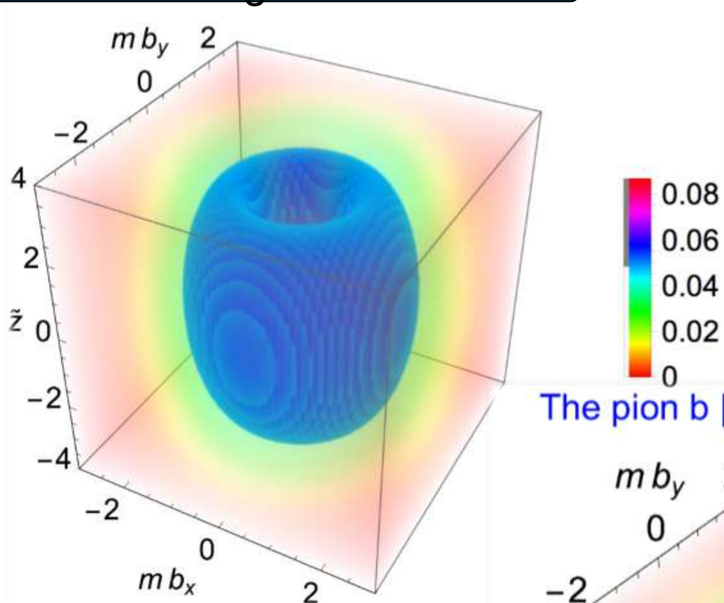

Aligned

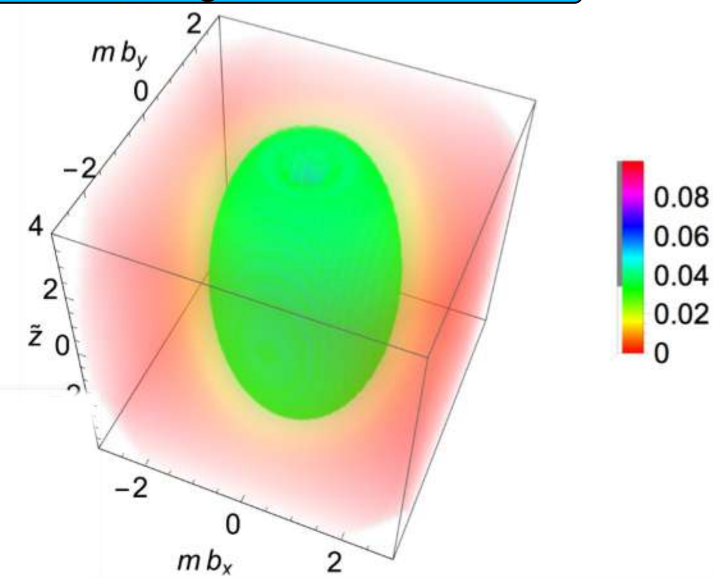

The pion b $|\psi|$^2 in the 3D Ioffe–space

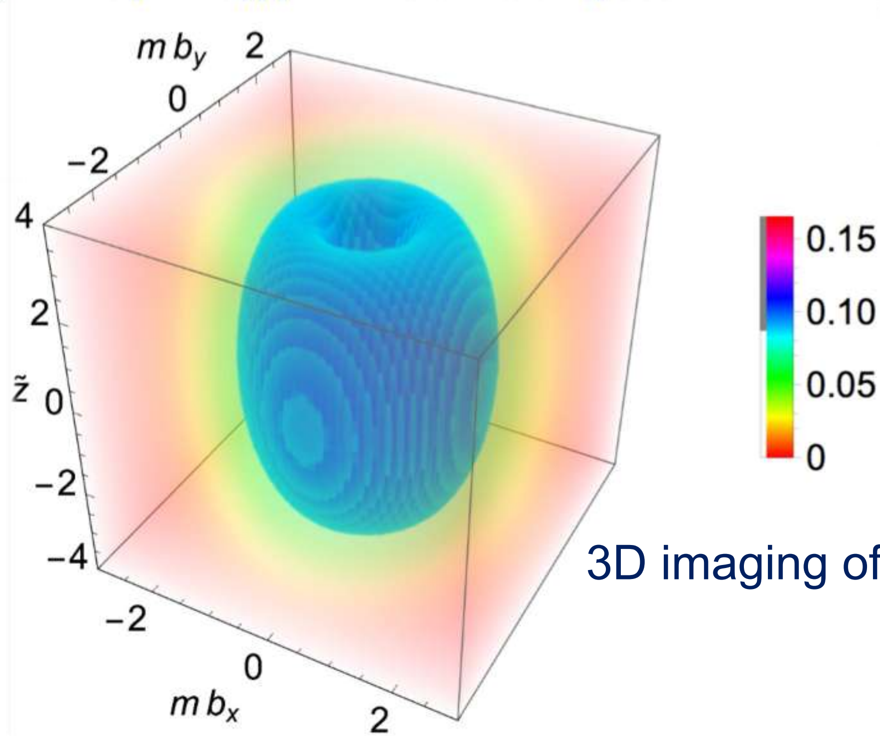

3D imaging of the Pion valence wf

Pion EM Form Factor

Alvarenga Nogueira, de Paula, TF, Ydrefors, Salmè, PLB *820, 136494 (2021)*

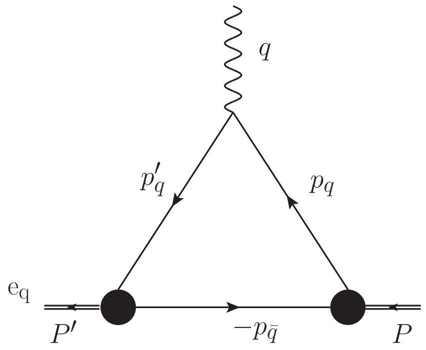

$$F(Q^2) = -i\,\frac{N_c}{M^2\,(1+\tau)}\int \frac{d^4 p_{\bar q}}{(2\pi)^4}\,\mathrm{Tr}\left[(-\not p_{\bar q} - m)\bar\Phi(k';P')(\not P + \not P')\;\Phi(k;P)\right]$$

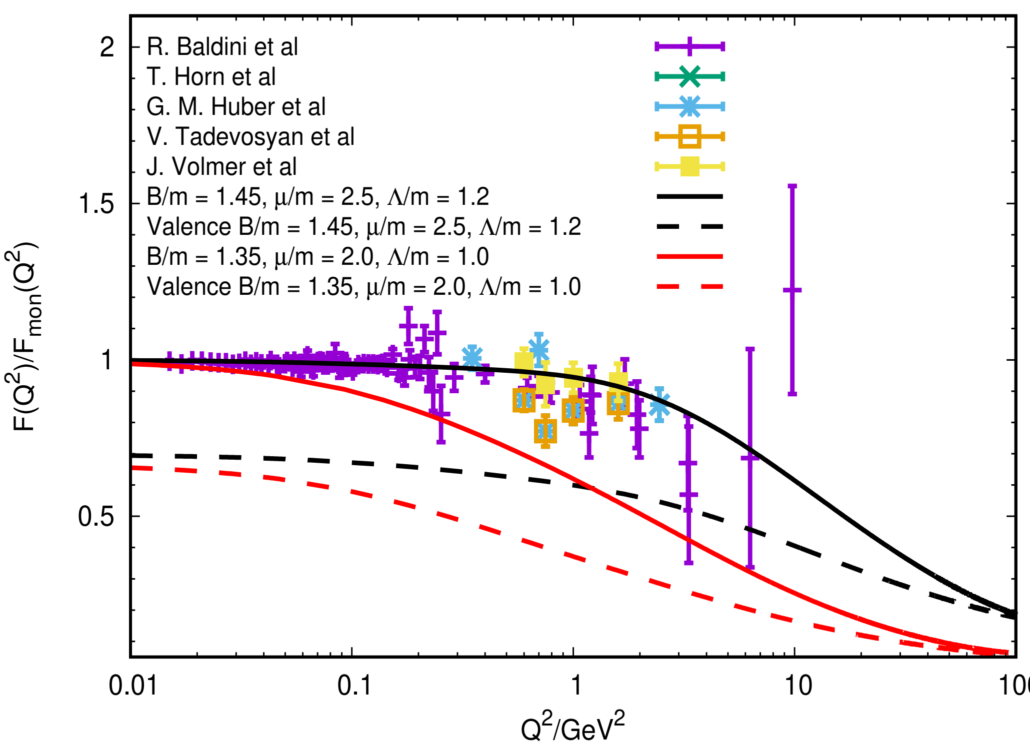

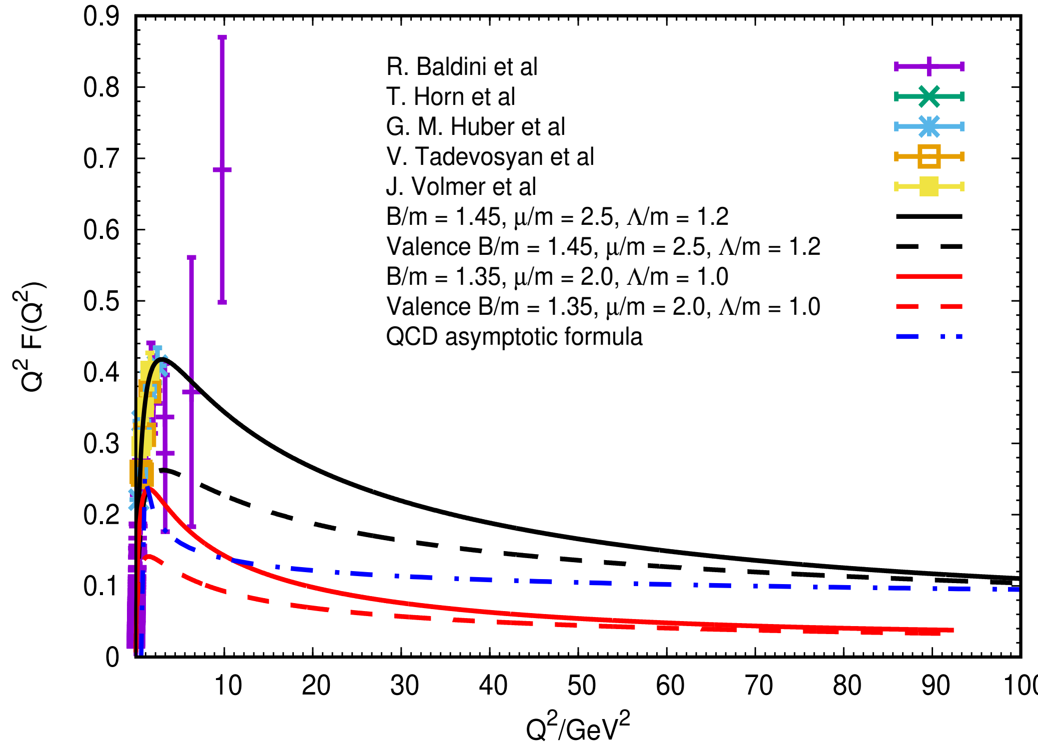

$$Q^2 F_{\rm asymp}(Q^2) = 8\pi\alpha_s(Q^2) f_\pi^2$$

G. Lepage, S. J. Brodsky, Phys. Lett. B 87 (1979) 359-

Decomposition of the pion EM form factor

$$\boxed{F_\pi(Q^2) = \sum_n \underset{\text{qq+gluons}}{F_n(Q^2)} = F_{val}(Q^2) + F_{nval}(Q^2)}$$

$$r_\pi^2 = P_{val}\, r_{val}^2 + (1 - P_{val})\, r_{nval}^2$$

r_π (fm)	r_{val} (fm)	r_{nval} (fm)
0.663	0.710	0.538

0.657 ± 0.003 fm B. Ananthanarayan, I. Caprini, D. Das, Phys. Rev. Lett. 119 (2017) 132002

70%

Valence

higher Fock-components → large virtuality → more compact

30%

The parton distribution function in a pion with Minkowskian dynamics

de Paula, Ydrefors, Alvarenga Nogueira, TF, Salmè, PRD 105, L071505 (2022)

T-even leading-twist (twist 2) - TMD (transverse-moment dependent) functions

$$f_1(\gamma,\xi) = \frac{N_c}{4}\int d\phi_{\hat{\mathbf{k}}_\perp}\int \frac{dz^- d\mathbf{z}_\perp}{2(2\pi)^3} e^{i[\xi P^+ z^-/2 - \mathbf{k}_\perp\cdot\mathbf{z}_\perp]} \langle P|\bar{\psi}_q(-\frac{1}{2}z)\gamma^+\psi_q(\frac{1}{2}z)|P\rangle\big|_{z^+=0} \quad \text{LC gauge}$$

$$\boxed{\begin{aligned} f_1(\gamma,\xi) = {} & \frac{1}{(2\pi)^4}\,\frac{1}{8}\int_{-\infty}^{\infty} dk^+\delta(k^+ + P^+/2 - \xi P^+)\int_{-\infty}^{\infty} dk^- \int_0^{2\pi} d\phi_{\hat{\mathbf{k}}_\perp} \\ & \times \left\{ Tr\left[S^{-1}(k-P/2)\bar{\Phi}(k,P)\,\frac{\gamma^+}{2}\,\Phi(k,P)\right] - Tr\left[S^{-1}(k+P/2)\Phi(k,P)\,\frac{\gamma^+}{2}\,\bar{\Phi}(k,P)\right]\right\} \end{aligned}}$$

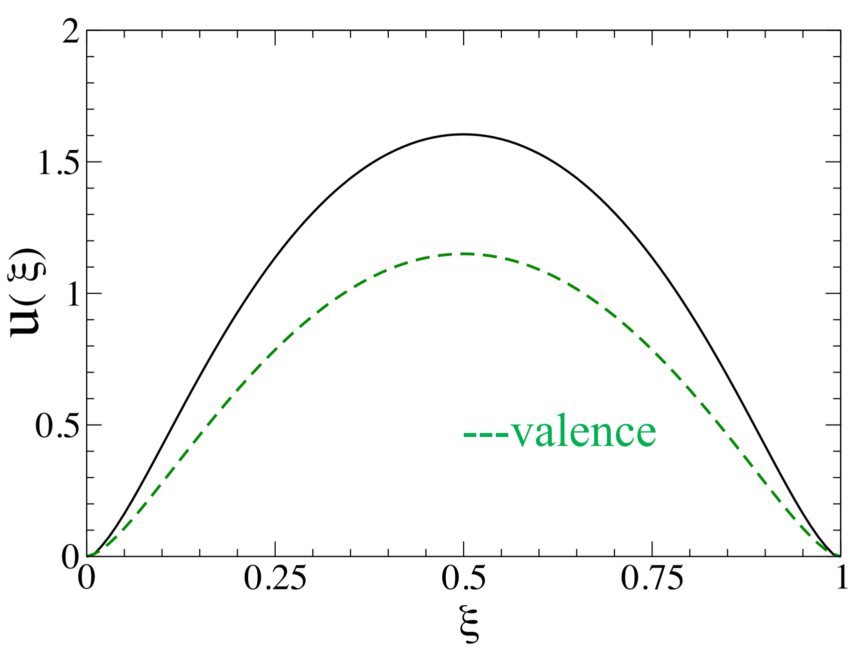

$$u(\xi) = \int_0^\infty d\gamma\ f_1(\gamma,\xi)$$

$$u_{val}(\xi) = \int_0^\infty \frac{d\gamma}{(4\pi)^2}\left[|\psi_{\uparrow\downarrow}(\gamma,z)|^2 + |\psi_{\uparrow\uparrow}(\gamma,z)|^2\right]$$

- Full PDF normalization is 1
- Valence PDF normalization is 0.7
- For $\xi \to 1$, PDF ~ $(1-\xi)^{\eta_0}$ $\eta_0 = 1.4$

Parton distribution function

WP, Ydrefors, Nogueira, Frederico and Salme PRD 105 L071505 (2022).

Low order Mellin moments at scales $Q = 2.0$ GeV and $Q = 5.2$ GeV.

	BSE_2	LQCD_2	BSE_5	LQCD_5
$\langle x\rangle$	0.259	0.261 ± 0.007	0.221	0.229 ± 0.008
$\langle x^2\rangle$	0.105	0.110 ± 0.014	0.082	0.087 ± 0.009
$\langle x^3\rangle$	0.052	0.024 ± 0.018	0.039	0.042 ± 0.010
$\langle x^4\rangle$	0.029		0.021	0.023 ± 0.009
$\langle x^5\rangle$	0.018		0.012	0.014 ± 0.007
$\langle x^6\rangle$	0.012		0.008	0.009 ± 0.005

LQCD, $Q = 2.0$ GeV: $\langle x\rangle$ - Alexandrou et al PRD 103, 014508 (2021)

$\langle x^2\rangle$ and $\langle x^3\rangle$ - Alexandrou et al PRD 104, 054504 (2021)

LQCD, $Q = 5.0$ GeV: $\langle x\rangle$ - Alexandrou et al PRD 103, 014508 (2021)

Hadronic scale and effective charge for DGLAP

$Q_0 = 0.330 \pm 0.030$ GeV - Cui et al EPJC 2020 80 1064

Within the error, we choose $Q_0 = 0.360$ GeV to fit the first Mellin moment.

We used lowest order DGLAP equations for evolution

Parton distribution function

WP, Ydrefors, Nogueira, Frederico and Salmè PRD 105, L071505 (2022).

Comparison with other theoretical calculations

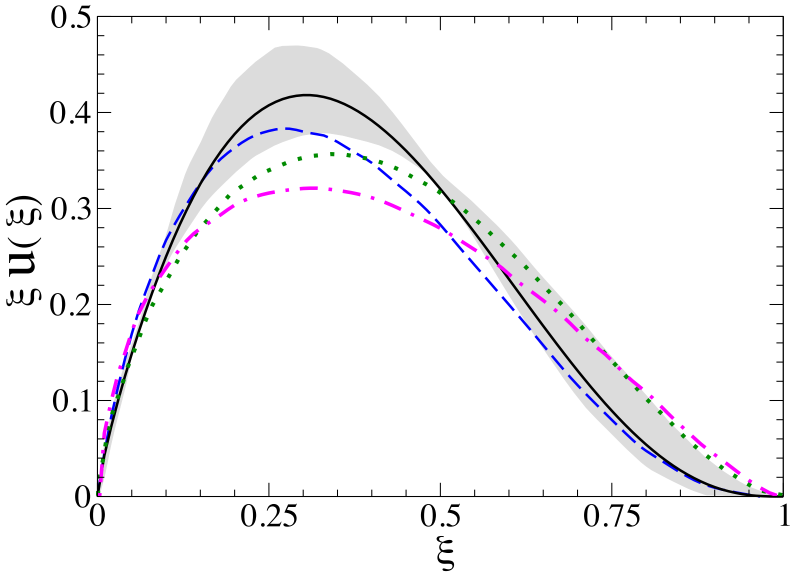

Solid line: full calculation of the BSE evolved

from the initial scale $Q_0 = 0.360$ GeV to $Q = 5.2$ GeV

Dashed line: DSE calculation (Cui et al)

Dash-dotted line: DSE calculation with dressed quark-photon vertex

from Bednar et al PRL 124, 042002 (2020)

Dotted line: BLFQ colaboration, PLB 825, 136890 (2022)

Gray area: LQCD results from C. Alexandrou et al (2021)

It is in agreement with PQCD, exponent greater than 2

Evolved $\xi\, u(\xi)$, for $\xi \to 1$, the exponent of $(1-\xi)^{\eta_5}$ is $\eta_5 = 2.94$

LQCD: Alexandrou et al PRD 104, 054504 (2021) obtained 2.20 ± 0.64

Cuit et al EPJA 58, 10 (2022) obtained 2.81 ± 0.08

Comparison with experimental data

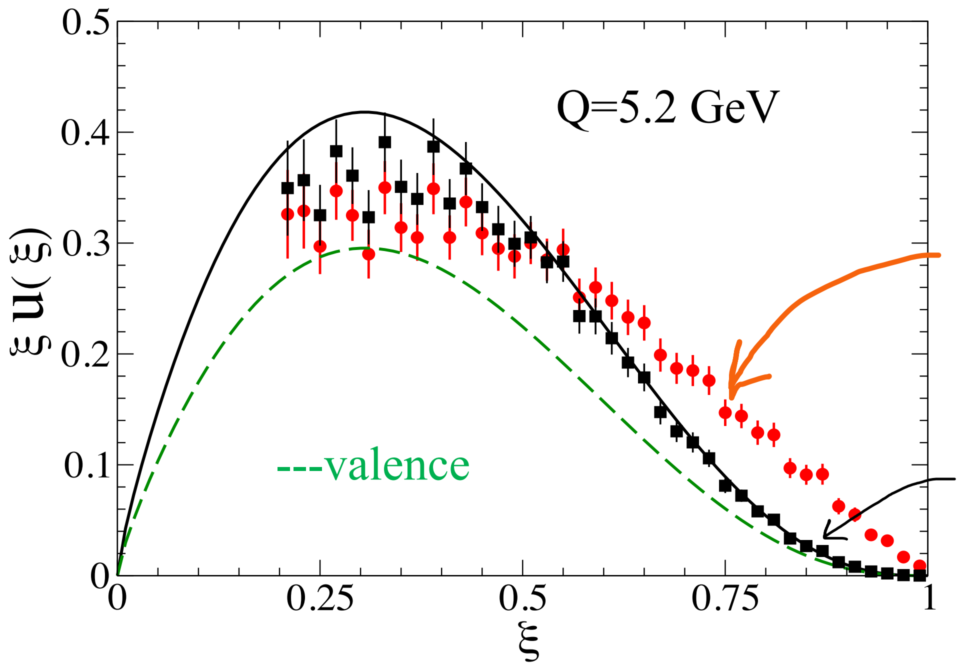

[32] J. Conway *et al.*, Experimental Study of Muon Pairs Produced by 252-GeV Pions on Tungsten, Phys. Rev. D **39**, 92 (1989).

[33] M. Aicher, A. Schäfer, and W. Vogelsang, Soft-gluon resummation and the valence parton distribution function of the pion, Phys. Rev. Lett. **105**, 252003 (2010), arXiv:1009.2481 [hep-ph].

FIG. 2. (Color online). The distribution function $\xi\ u(\xi)$ in a pion. Solid line: full calculation (see Eqs. (7) and (8)), obtained from the BS amplitude solution of the BSE with $m = 255$ MeV, $\mu = 637.5$ MeV and $\Lambda = 306$ MeV, and evolved from the initial scale $Q_0 = 0.360$ GeV to $Q = 5.2$ GeV (see text). Dashed line: the evolved LF valence component, Eq. (9). Full dots: experimental data from Ref. [32]. Full squares: reanalyzed data by using the ratio between the fit 3 of Ref. [33], evolved to 5.2 GeV, and the experimental data [32], at each data point, so that the resummation effects (see text) are accounted for.

Quark unpolarized transverse-momentum distribution functions of the pion

Ydrefors, de Paula, TF, Salmè, e-Print: 2301.11599 [hep-ph]

T-even uTMD leading-twist from the quark-quark correlator
Mulders & Tangerman NPB461, 197 (1996)

$$f_1^q(\gamma,\xi) = \frac{N_c}{4}\int d\phi_{\hat{\mathbf{k}}_\perp}\int_{-\infty}^{\infty}\frac{dy^- d\mathbf{y}_\perp}{2(2\pi)^3} \times e^{i[\xi P^+ \frac{y^-}{2} - \mathbf{k}_\perp\cdot\mathbf{y}_\perp]}\langle P|\bar{\psi}_q(-\tfrac{y}{2})\gamma^+\psi_q(\tfrac{y}{2})|P\rangle\Big|_{y^+=0}$$

$$\gamma = |\mathbf{k}_\perp|^2$$

$$f_1^q(\gamma,\xi) = \frac{N_c}{4(2\pi)^3}\int_{-\infty}^{\infty}\frac{dk^+}{2(2\pi)}\delta\Big(k^+ + \frac{P^+}{2} - \xi P^+\Big) \times \int_{-\infty}^{\infty}dk^- \int_0^{2\pi} d\phi_{\hat{\mathbf{k}}_\perp}\mathrm{Tr}\left[S^{-1}(-p_{\bar{q}})\bar{\Phi}(k,P)\,\gamma^+\,\Phi(k,P)\right]$$

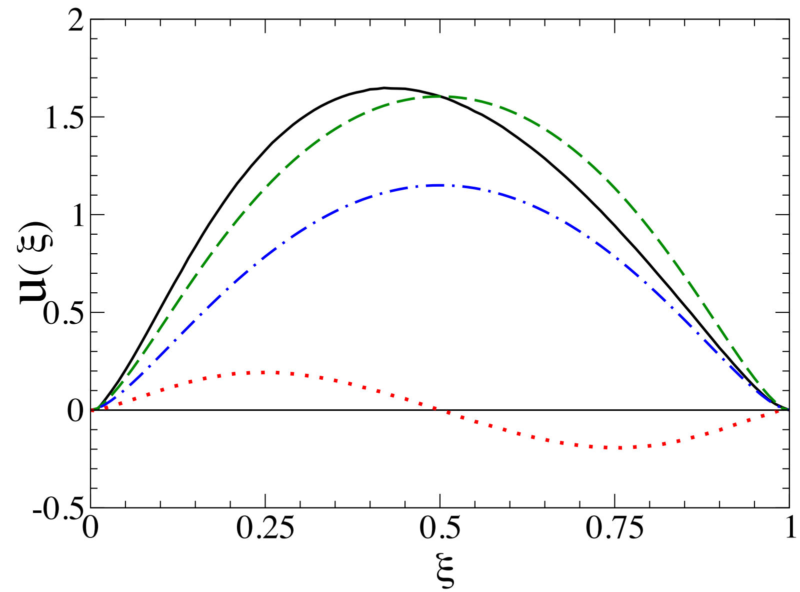

$$\langle\xi_q\rangle = \int_0^1 d\xi\int_0^\infty d\gamma\ \xi\ f_1^q(\gamma,\xi) = 0.471$$

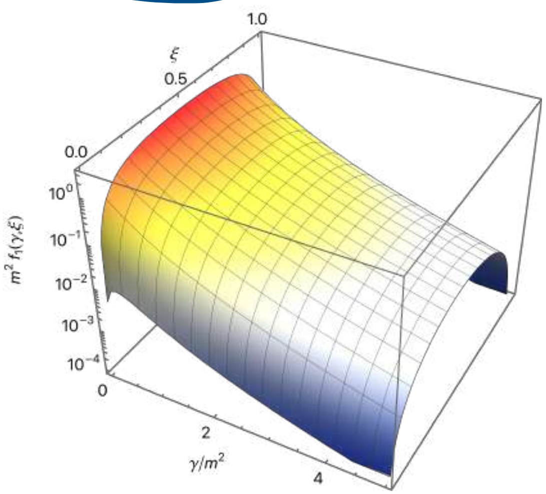

$$|\pi\rangle = |q\bar{q}\rangle + |q\bar{q}g\rangle + |q\bar{q}\,2g\rangle + \cdots$$

Bethe-Salpeter amplitude: beyond the valence states

Light-front projection

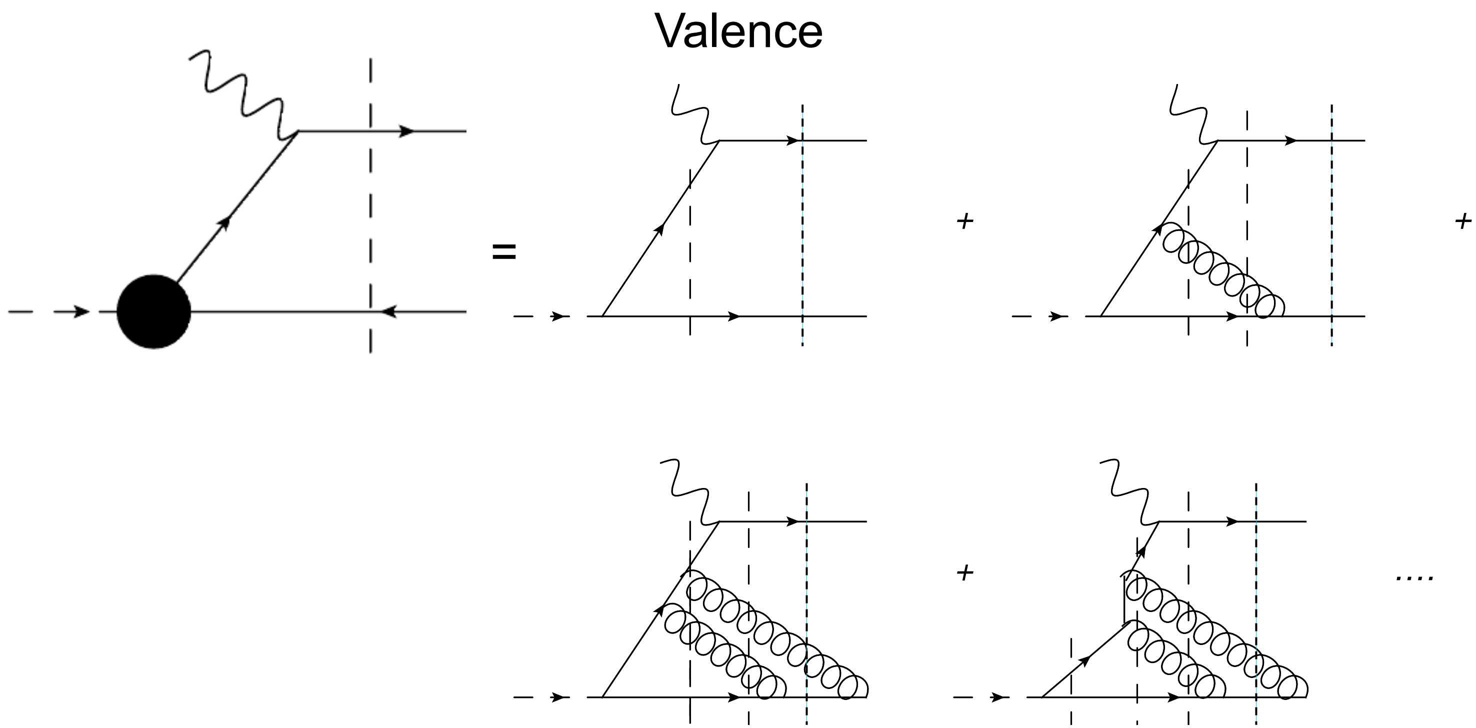

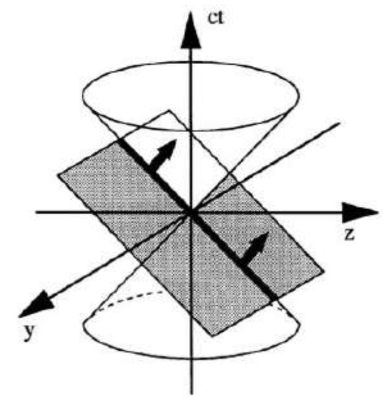

- **higher Fock-components** $|\pi\rangle = |q\bar{q}\rangle + |q\bar{q}g\rangle + |q\bar{q}\,2g\rangle + \cdots$
- **gluon radiation from initial state interaction (ISI)**
- **No gluon radiation in the final state (FSI)**

Sales, TF, Carlson,Sauer, PRC 63, 064003 (2001); Marinho, TF, Pace,Salme,Sauer, PRD 77, 116010 (2008)

Gluon momentum in the pion

$$|\pi\rangle = |q\bar{q}\rangle + |q\bar{q}g\rangle + |q\bar{q}\,2g\rangle + \cdots$$

quark momentum distribution

$$u^q(\xi) = \sum_{n=2}^{\infty} \left\{ \prod_i^n \int \frac{d^2 k_{i\perp}}{(2\pi)^2} \int_0^1 d\xi_i \right\}$$
$$\times \delta\left(\xi - \xi_1\right) \delta\left(1 - \sum_{i=1}^n \xi_i\right) \delta\left(\sum_{i=1}^n \mathbf{k}_{i\perp}\right)$$
$$\times \left|\Psi_n(\xi_1, \mathbf{k}_{1\perp}, \xi_2, \mathbf{k}_{2\perp}, \ldots)\right|^2,$$

first-moment

$$\langle \xi_q \rangle = P_{val}\ \langle \xi_q \rangle_{val} + \sum_{n>2} P_n\ \langle \xi_q \rangle_n$$

0.471 0.5

$$= P_{val}\ \langle \xi_q \rangle_{val} + (1 - P_{val})\ \langle \xi_q \rangle_{HFS}$$

0.4

P_{val}=0.3

momentum sum-rule in the HFS

$$\langle \xi_q \rangle_{HFS} = 1 - \langle \xi_{\bar{q}} \rangle_{HFS} - \langle \xi_g \rangle$$

0.2

Gluons carry 6% of the longitudinal momentum of the pion!

@ the pion scale

Transverse Momentum Distributions

Unpolarized transverse-momentum dependent quark distributions

TMD's are important for parametrizing the hadronic quark-quark correlator

One can define the T-even subleading quark uTMDs, starting from the decomposition of the pion correlator (Mulders and Tangerman, Nucl. Phys. B 461, 197 (1996)).

twist-3 uTMD (See Lorcé, Pasquini, and Schweitzer, EPJC 76, 415 (2016)):

$$\frac{M}{P^+}\ e^q(\gamma,\xi) = \frac{N_c}{4}\int d\phi_{\hat{\mathbf{k}}_\perp}\int_{-\infty}^{\infty}\frac{dy^-\, d\mathbf{y}_\perp}{2(2\pi)^3}\ e^{i[\xi P^+ y^-/2 - \mathbf{k}_\perp\cdot\mathbf{y}_\perp]}\ \langle P|\bar{\psi}_q(-\frac{y}{2})\ \hat{1}\ \psi_q(\frac{y}{2})|P\rangle\big|_{y^+=0}$$

$$\frac{M}{P^+}\ f^{\perp q}(\gamma,\xi) = \frac{N_c M}{4\gamma}\int d\phi_{\hat{\mathbf{k}}_\perp}\int_{-\infty}^{\infty}\frac{dy^-\, d\mathbf{y}_\perp}{2(2\pi)^3}\ e^{i[\xi P^+ y^-/2 - \mathbf{k}_\perp\cdot\mathbf{y}_\perp]}\ \langle P|\bar{\psi}_q(-\frac{y}{2})\ \mathbf{k}_\perp\cdot\boldsymbol{\gamma}_\perp\ \psi_q(\frac{y}{2})|P\rangle\big|_{y^+=0}$$

$$\gamma = |\mathbf{k}_\perp|^2$$

Subleading-twist 3 uTMDs

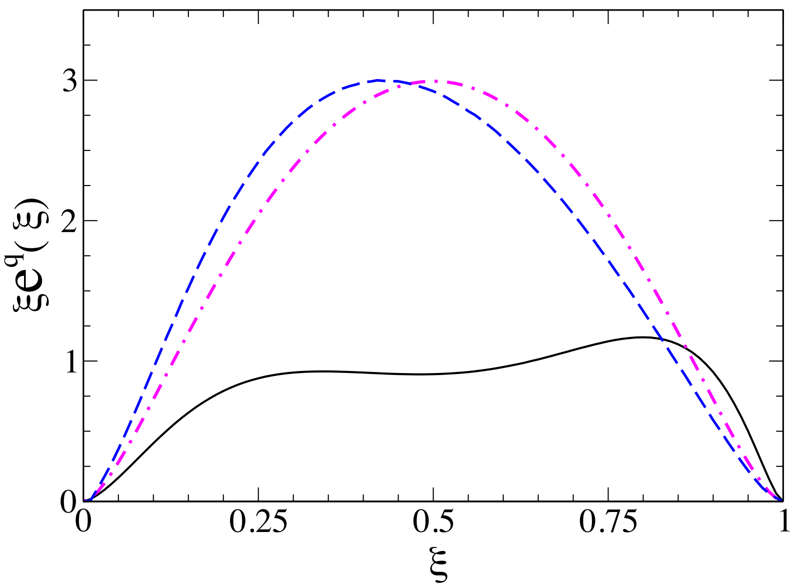

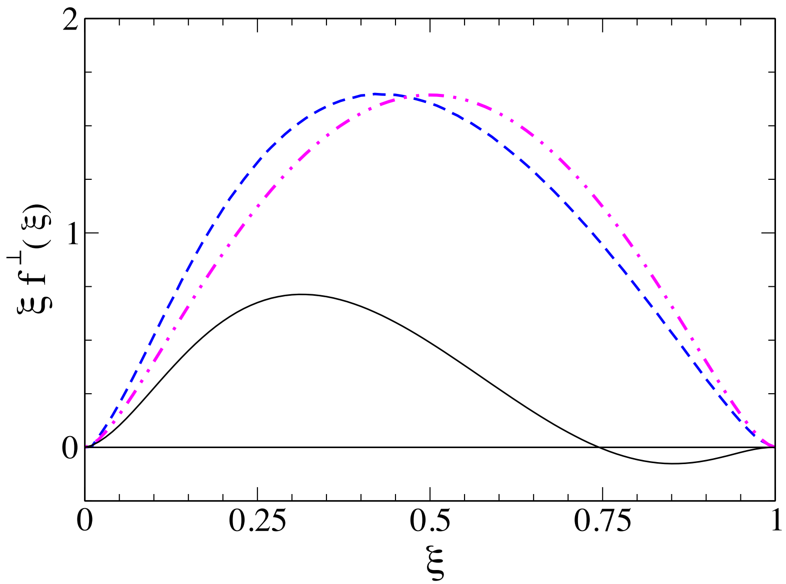

$$\xi \; e^q_{EoM}(\gamma,\xi) = \xi \; \tilde{e}^q(\gamma,\xi) + \frac{m}{M} \; f^q_{1;EoM}(\gamma,\xi)$$

$$\xi \; f^{q\perp}_{EoM}(\gamma,\xi) = \xi \; \tilde{f}^{q\perp}(\gamma,\xi) + f^q_{1;EoM}(\gamma,\xi) \; ,$$

$$\gamma = |\mathbf{k}_\perp|^2$$

Lorcé, Pasquini, Schweitzer, EPJ C 76, 415 (2016)

PION MODEL FROM LQCD RUNNING QUAK MASS

C.S. Mello et al. / Physics Letters B 766 (2017) 86-

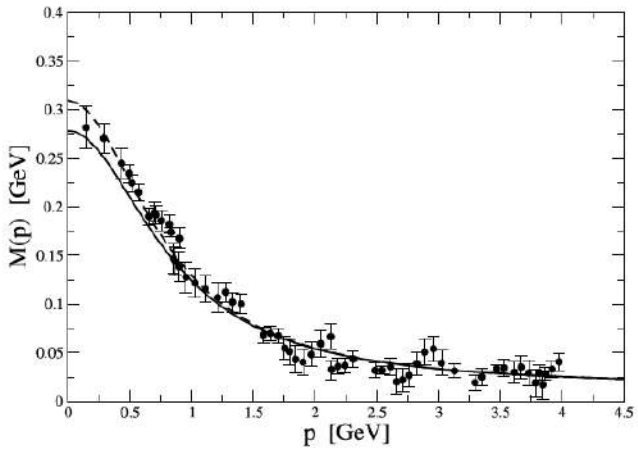

Fig. 1. The running quark mass, Eq. (3), as a function of the Euclidean momentum $p = \sqrt{-p^\mu p_\mu}$, with parameters from (4), is given by the solid line and compared to lattice QCD calculations from [37]. The dashed line shows the parametrization used in reference [51].

$$S_F(k) = \imath \left[\not{k} - M(k^2) + \imath\epsilon \right]^{-1}$$

$$M(k^2) = m_0 - m^3 \left[k^2 - \lambda^2 + i\epsilon \right]^{-1}$$

$$m_0 = 0.014\,\text{GeV}, \;\; m = 0.574\,\text{GeV and } \lambda = 0.846\,\text{GeV}$$

$$\psi_\pi(k; P) = S_F(k + P/2)\,\Gamma_\pi(k; P)\,S_F(k - P/2)$$

$$\Gamma_\pi(k; P) = \imath\,\mathcal{N}\,\gamma_5\,M(k^2)|_{m_0=0}$$

$$\Phi(k,p) = S_1\phi_1 + S_2\phi_2 + S_3\phi_3 + S_4\phi_4$$

$$S_1 = \gamma_5 \quad S_2 = \frac{1}{M}\not{p}\gamma_5 \quad S_3 = \frac{k\cdot p}{M^3}\not{p}\gamma_5 - \frac{1}{M}\not{k}\gamma_5 \quad S_4 = \frac{i}{M^2}\sigma_{\mu\nu}p^\mu k^\nu\gamma_5$$

$$\phi_i(k,p) = \int_{-1}^{1} dz' \int_{-\infty}^{\infty} d\gamma' \frac{g_i(\gamma', z')}{[k^2 + z'k\cdot p - \gamma' + \imath\epsilon]^3}.$$

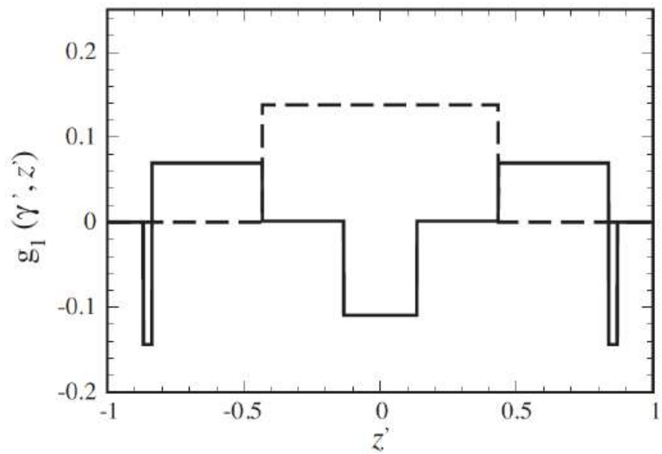

FIG. 5. Weight function $g_1(\gamma, z)$ as a function of z for $\gamma = 0.45\ \mathrm{GeV}^2$ coming from the covariant model with fixed constituent mass (dashed line) and with the QCD pion inspired model (the single constituent mass pole model has $g_3 = 0$). For the plot, we use the arbitrary value of $\mathcal{N} = 100$, drop out the factor of i and all parameters are in units of GeV.

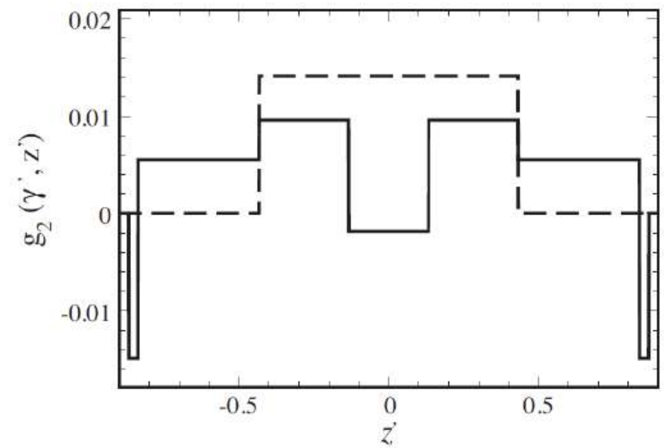

FIG. 6. Weight function $g_2(\gamma, z)$ as a function of z for $\gamma = 0.45\ \mathrm{GeV}^2$ coming from the covariant model with fixed constituent mass (dashed line) and with the QCD pion inspired model (continuous line). For the plot, we use the arbitrary value of $\mathcal{N} = 100$, drop out the factor of i and all parameters are in units of GeV.

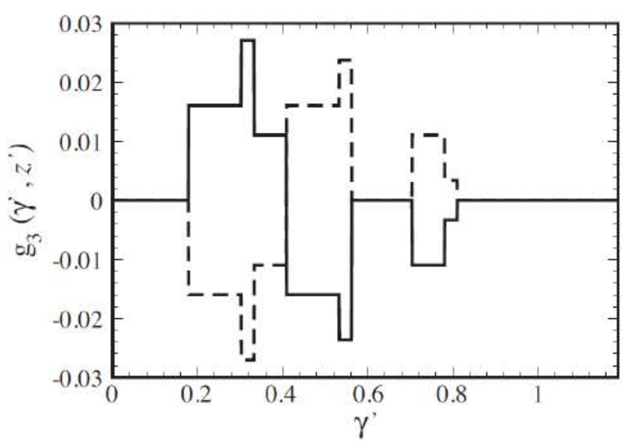

FIG. 7. Weight function $g_3(\gamma, z)$ as a function of γ computed with the QCD pion inspired model for $z = 0.5$ (continuous line) and for $z = -0.5$ (dashed line). For the plot, we use the arbitrary value of $\mathcal{N} = 100$, drop out the factor of i and all parameters are in units of GeV.

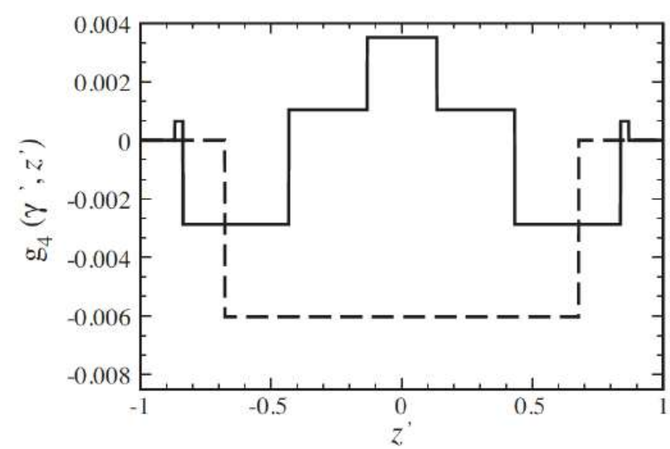

FIG. 8. Weight function $g_4(\gamma, z)$ as a function of z for $\gamma = 0.45\ \mathrm{GeV}^2$ coming from the covariant model with fixed constituent mass (dashed line) and with the QCD pion inspired model (continuous line). For the plot, we use the arbitrary value of $\mathcal{N} = 100$, drop out the factor of i and all parameters are in units of GeV.

Moita, de Melo, TF, de Paula, PRD 106, 016016 (2022)

P_{val}	$P_{\uparrow\downarrow}$	$P_{\uparrow\uparrow}$	f_π(MeV)
0.70	0.58	0.12	130.1

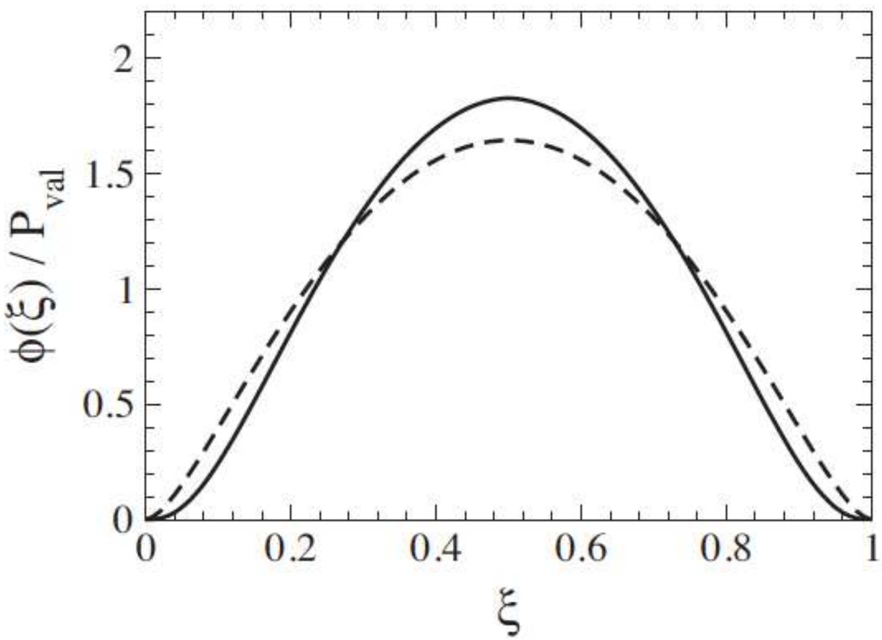

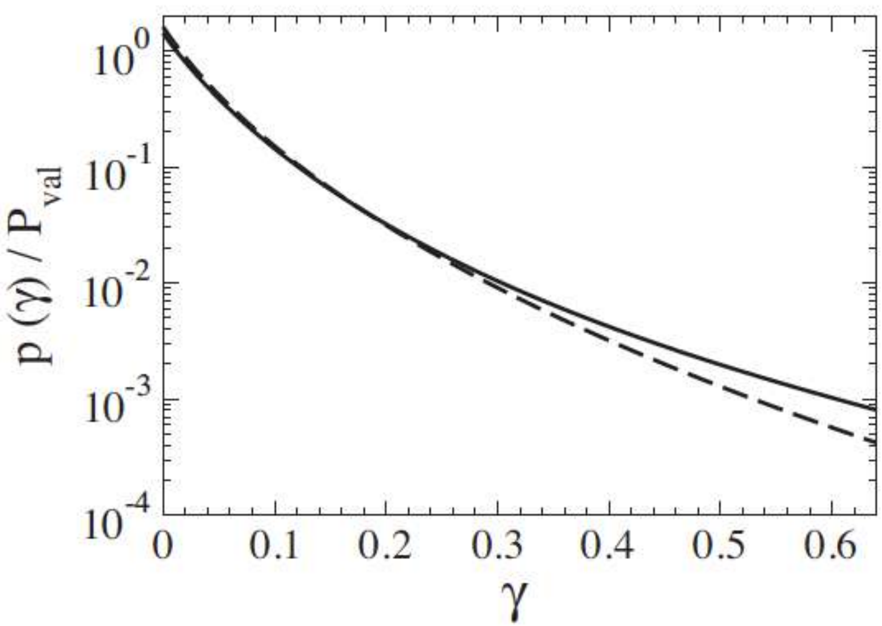

Kekez and Klabucar, arXiv:2006.02326v1 [hep-ph]

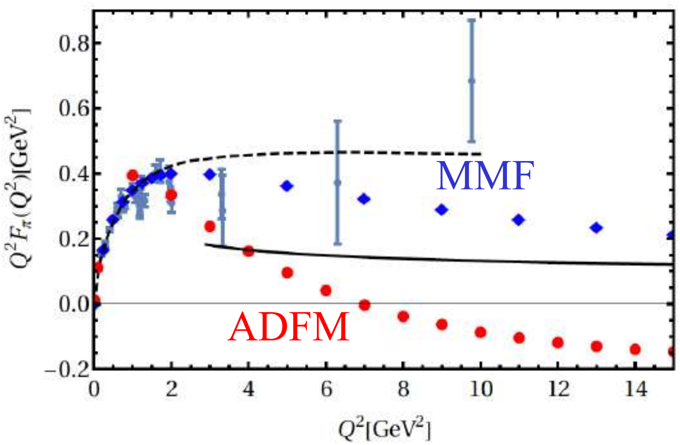

FIG. 5. (color online). Charged pion electromagnetic form factor. Experimental points are a compilation adopted from Ref. [56]. Red solid circles and blue diamonds are calculated using the ADFM quark propagator *Ansatz* and the MMF quark propagator *Ansatz*, respectively. In the both cases, three different methods of calculation (detailed in the text) yielded the same results. Black dashed line represents the result of Mello *et al.* [32]. Black solid line corresponds to the perturbative QCD result (27) with asymptotic PDA.

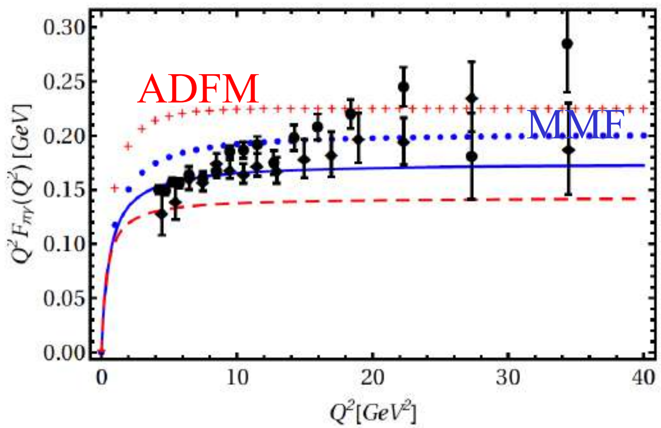

FIG. 7. (color online). Blue dots represent π^0 transition form factor calculated using the MMF quark propagator *Ansatz*, Eqs. (1) and (2). The red pluses are calculated using the ADFM quark propagator, Eqs. (6). The blue solid line and red dashed line represent the Brodsky–Lepage interpolation formula, Eq. (29), for the MMF quark propagator and ADFM quark propagator models, respectively. Solid circles and diamonds (with error bars) represent the measurements of BaBar [62] and Belle [63] collaboration, respectively.

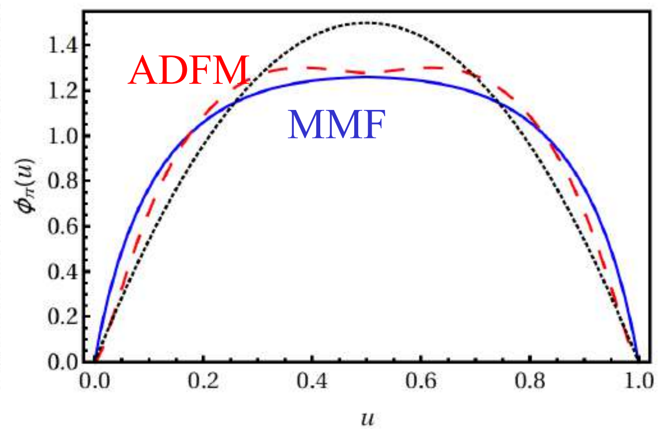

FIG. 8. (color online). Pion distribution amplitudes $\phi_\pi(u)$. Blue solid line and red dashed line correspond to the MMF and ADFM *Ansätze*, respectively. Black dotted line represents the asymptotic form, $\phi_\pi^{\rm as}(u) = 6u(1-u)$.

(MMF) Mello, de Melo, Frederico, PLB766, 86 (2017)

(ADFM) Alkofer, Detmold, Fischer, Maris, PRD70, 014014 (2004)

PION DYNAMICS & QUAK SELF ENERGY

0^- Bound State with Running quark mass function

Abigail Castro, WP, Ydrefors, Frederico, Salmè - in preparation

Dressed quark propagator: $S(p) = i\,Z(p^2)\,\frac{\not{p}+\mathcal{M}(p^2)}{p^2-\mathcal{M}^2(p^2)}$

Phenomenological model to reproduce Lattice Data for $\mathcal{M}(p^2)$ *(Mello, de Melo, Frederico, PLB 766, 86 (2017))*:

$$\mathcal{M}(p^2) = m_0 - \frac{m^3}{p^2 - \lambda^2 + i\epsilon}$$

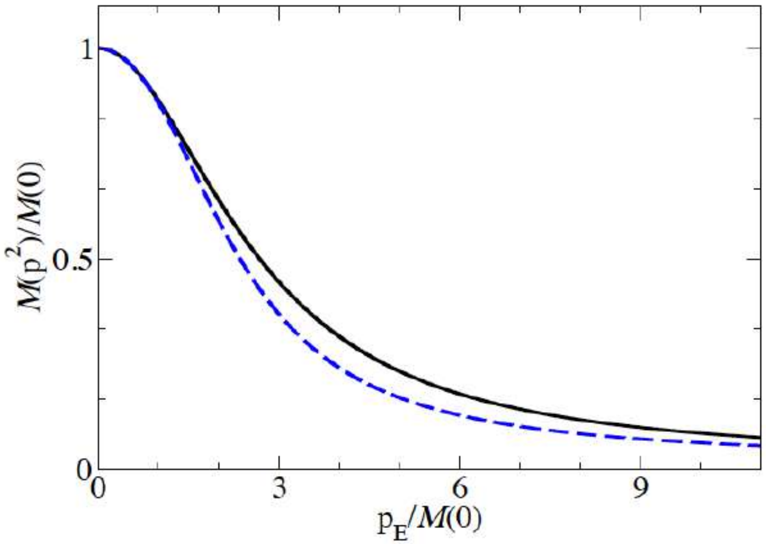

From Lattice simulations: bare quark mass $m_0 = 8\,\mathrm{MeV}$ and $\mathcal{M}(0) = 0.344$ GeV.
Our fit (solid line): $m = 0.648\,\mathrm{GeV}$ and $\lambda = 0.9\,\mathrm{GeV}$.

Lattice data (dashed line) from: Oliveira, Silva, Skullerud and Sternbec, PRD 99 (2019) 094506

0^- Bound State with Running quark mass function

Abigail Castro, WP, Ydrefors, Frederico, Salmè - $S^V(p^2) = \int_0^\infty ds \frac{\rho^V(s)}{p^2 - s + i\epsilon}$; $S^S(p^2) = \int_0^\infty ds \frac{\rho^S(s)}{p^2 - s + i\epsilon}$

Phenomenological model: $\mathcal{M}(p^2) = m_0 - \frac{m^3}{p^2 - \lambda^2 + i\epsilon}$

$$\rho^{S(V)}(s) = \sum_{a=1}^{3} R_a^{S(V)} \delta(s - m_a^2) \ ,$$

where $R_a^{S(V)}$ are the residues, that read

$$R_a^V = \frac{(\lambda^2 - m_a^2)^2}{(m_a^2 - m_b^2)(m_a^2 - m_c^2)} \ ,$$
$$R_a^S = R_a^V \ \mathcal{M}(m_a^2),$$

with the indices $\{a, b, c\}$ following the cyclic permutation $\{1, 2, 3\}$.

$\mathcal{M}(0)$ [GeV]	i	m_i [GeV]	R_i^V	R_i^S [GeV]
	1	0.4696	3.7784	1.7743
0.344	2	0.5733	-2.8863	-1.6546
	3	1.0349	0.1079	-0.1116

0^- Bound State with Running quark mass function

Abigail Castro, WP, Ydrefors, Frederico, Salmè - in preparation

Integral Representation: $S^V(p^2) = \int_0^\infty ds \frac{\rho^V(s)}{p^2-s+i\epsilon}$; $S^S(p^2) = \int_0^\infty ds \frac{\rho^S(s)}{p^2-s+i\epsilon}$

Using the Nakanishi integral representation for $\phi_i(k,p)$, performing the loop integral and projecting onto the LF, one obtains the BSE as

$$\int_0^\infty d\gamma' \frac{g_i(\gamma',z)}{\left[\gamma + z^2M^2/4 + \gamma' + \kappa^2 - i\epsilon\right]^2} = \frac{\alpha}{2\pi} \times \sum_j \int_{-1}^1 dz' \int_0^\infty d\gamma' \mathcal{L}_{ij}(\gamma,z;\gamma',z')\, g_j(\gamma',z') \, .$$

Longitudinal momentum distribution

Abigail Castro, WP, Ydrefors, Frederico, Salmè - in preparation

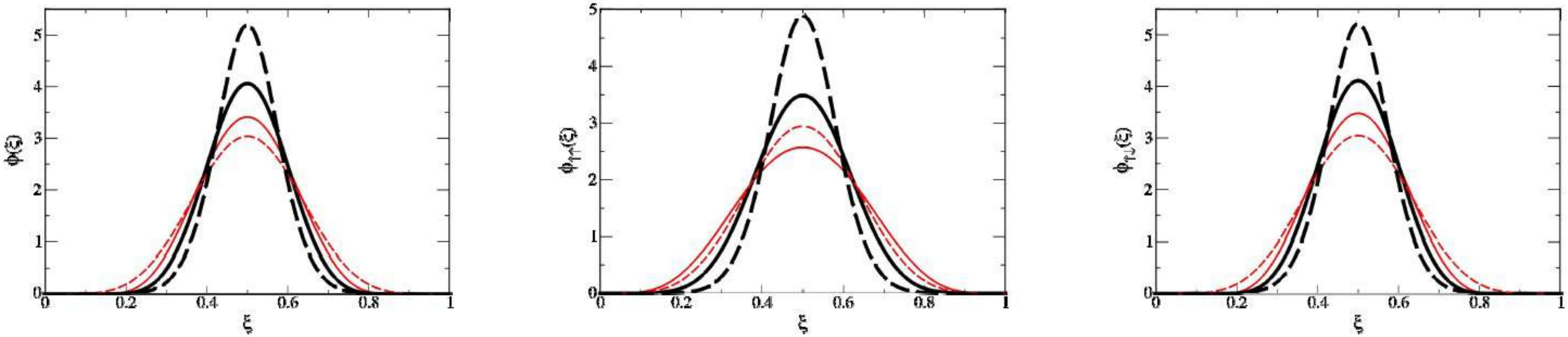

Transverse momentum distribution

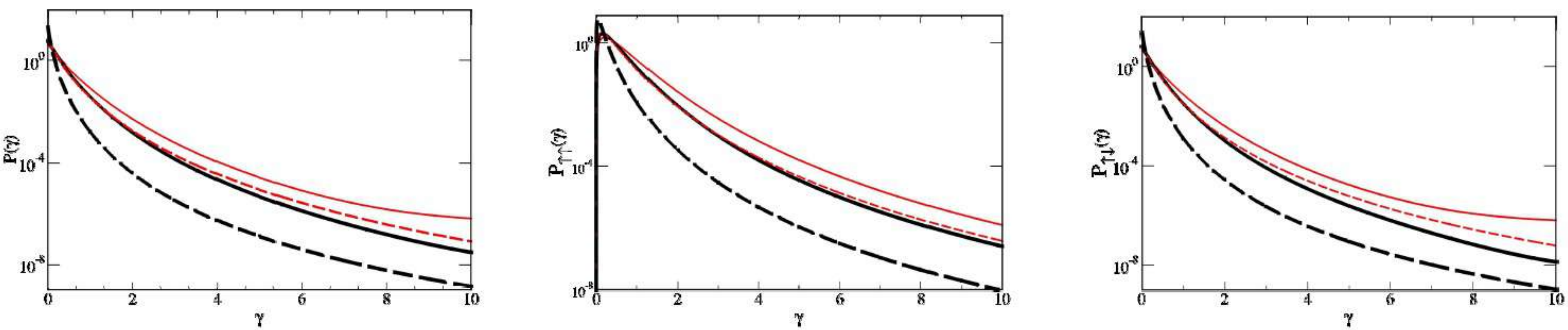

Parameters: $\Lambda = 0.12\,\text{GeV}$, $\mu = 0.469\,\text{GeV}$.

Thick solid line: running mass model for $M = 0.653$ GeV.

Thick dashed Line: fixed quark mass (344 MeV) for $M = 0.653$ GeV.

Thin solid line: running mass model for $M = 0.516\,\text{GeV}$.

Thin dashed line: fixed quark mass (344 MeV) for $M = 0.516\,\text{GeV}$.

Dressing the Quark: Schwinger-Dyson equation

The model: Bare vertices, massive vector boson, Pauli-Villars regulator

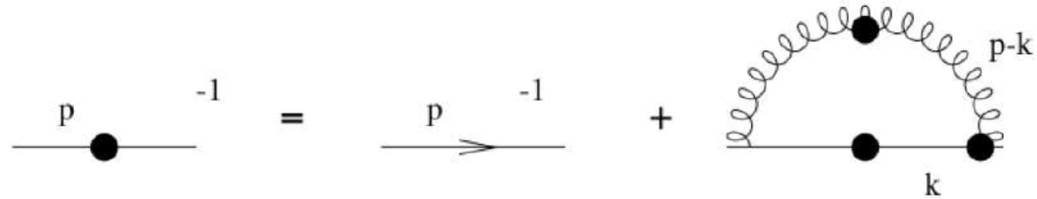

Credits to Wayne de Paula

The rainbow ladder Schwinger-Dyson equation in Minkowski space is:

$$S_q^{-1}(k) = \not{k} - m_B + ig^2 \int \frac{d^4 q}{(2\pi)^4} \Gamma_\mu(q,k) S_q(k-q) \gamma_\nu D^{\mu\nu}(q) \,,$$

where m_B is the quark bare mass and g is the coupling constant.
The massive gauge boson is given by

$$D^{\mu\nu}(q) = \frac{1}{q^2 - m_g^2 + \imath\epsilon} \left[g^{\mu\nu} - \frac{(1-\xi) q^\mu q^\nu}{q^2 - \xi m_g^2 + \imath\epsilon} \right] \,,$$

where we have introduce an effective gluon mass m_g, as suggested by LQCD calculations (*see Dudal, Oliveira and Silva, PRD 89 (2014) 014010*).
The dressed fermion propagator is

$$S_q(k) = \left[\not{k} A(k^2) - B(k^2) + i\epsilon \right]^{-1} .$$

Duarte, TF, de Paula, Ydrefors, PRD105, 114055 (2022)

Schwinger-Dyson equation in Rainbow ladder truncation

The vector and scalar self-energies are given by the NIR, respectively as:

$$
\begin{aligned}
A\left(k^2\right) &= 1+\int_0^\infty ds \frac{\rho_A\left(s\right)}{k^2-s+i\epsilon}\,, \\
B\left(k^2\right) &= m_B+\int_0^\infty ds \frac{\rho_B\left(s\right)}{k^2-s+i\epsilon}\,.
\end{aligned}
$$

The quark propagator can also be written as:

$$
S_q(k) = R\frac{\not{k}+\overline{m}_0}{k^2-\overline{m}_0^2+i\epsilon}+\not{k}\int_0^\infty ds \frac{\rho_v\left(s\right)}{k^2-s+i\epsilon}+\int_0^\infty ds \frac{\rho_s\left(s\right)}{k^2-s+i\epsilon}\,,
$$

where $\overline{m}_0$ is the renormalized mass.

Gauge fixing

$$
\begin{aligned}
\not{k}A(k^2)-B(k^2) = {} & ig^2\int \frac{d^4q}{(2\pi)^4}\frac{\gamma_\mu S_f(k-q)\gamma_\nu}{q^2-m_g^2+i\epsilon}\left[g^{\mu\nu}-\frac{(1-\xi)\,q^\mu q^\nu}{q^2-\xi m_g^2+i\epsilon}\right] \\
& -i\,g^2\int \frac{d^4q}{(2\pi)^4}\frac{\gamma_\mu S_f(k-q)\gamma_\nu}{q^2-\Lambda^2+i\epsilon}\left[g^{\mu\nu}-\frac{(1-\xi)q^\mu q^\nu}{q^2-\xi\Lambda^2+i\epsilon}\right]
\end{aligned}
$$

Pauli-Villars regulator

Fermion Schwinger-Dyson equation

- Parameters: $\alpha = \dfrac{g^2}{4\pi}$, Λ , m_g , $\overline{m}_0$.

- Spectral densities are obtained from the IR of the self-energy:

$$\rho_A(\gamma) = -\frac{1}{\pi}\mathrm{Im}\left[A(\gamma)\right]$$
$$\rho_B(\gamma) = -\frac{1}{\pi}\mathrm{Im}\left[B(\gamma)\right]$$

- Solutions of DSE obtained writing the trivial relation $S_f^{-1}S_f = 1$ in a suitable form:

$$\frac{R}{\gamma - \overline{m}_0^2 + \imath\epsilon} + \int_0^\infty ds \frac{\rho_v(s)}{\gamma - s + i\epsilon} = \frac{A(\gamma)}{\gamma A^2(\gamma) - B^2(\gamma) + i\epsilon}$$
$$\frac{R\,\overline{m}_0}{\gamma - \overline{m}_0^2 + i\epsilon} + \int_0^\infty ds \frac{\rho_s(s)}{\gamma - s + i\epsilon} = \frac{B(\gamma)}{\gamma A^2(\gamma) - B^2(\gamma) + i\epsilon}$$

Fermion Schwinger-Dyson equation

$$\rho_A(\gamma) = R\mathcal{K}^{\xi}_{0A}(\gamma, \overline{m}_0^2, m_g^2) + \int_0^{\infty} ds\, \mathcal{K}^{\xi}_A(\gamma, s, m_g^2)\, \rho_v(s) - [m_g \to \Lambda]$$

$$\rho_B(\gamma) = R\,\overline{m}_0\, \mathcal{K}^{\xi}_{0B}(\gamma, \overline{m}_0^2, m_g^2) + \int_0^{\infty} ds\, \mathcal{K}^{\xi}_B(\gamma, s, m_g^2)\, \rho_s(s) - [m_g \to \Lambda]$$

- Driving term:

$$\mathcal{K}^{\xi}_{0A(0B)} = K_{A(B)} + m_g^{-2} \bar{K}^{\xi}_{A(B)}$$

- Kernel:

$$\mathcal{K}^{\xi}_A(\gamma, s, m_g^2) = K_A(\gamma, s, m_g^2)\, \Theta(s - (\overline{m}_0 + m_g)^2) + m_g^{-2} \bar{K}^{\xi}_A(\gamma, s, m_g^2)\, \Theta(s - (\overline{m}_0 + \sqrt{\xi} m_g)^2)$$

$$f_A(\gamma) = 1 + \int_0^{\infty} ds \frac{\rho_A(s)}{\gamma - s}$$

$$f_B(\gamma) = m_B + \int_0^{\infty} ds \frac{\rho_B(s)}{\gamma - s}$$

$$d(\gamma) = \left[\gamma f_A^2(\gamma) - \pi^2\, \gamma\, \rho_A^2(\gamma) - f_B^2(\gamma) + \pi^2\, \rho_B^2(\gamma)\right]^2 + 4\pi^2 \left[\gamma \rho_A(\gamma)\, f_A(\gamma) - \rho_B(\gamma)\, f_B(\gamma)\right]^2$$

Connection Formulas

$$\rho_v(\gamma) = -2\frac{f_A(\gamma)}{d(\gamma)} \left[\gamma \rho_A(\gamma)\, f_A(\gamma) - \rho_B(\gamma)\, f_B(\gamma)\right] + \frac{\rho_A(\gamma)}{d(\gamma)} \left[\gamma\, f_A^2(\gamma) - \pi^2 \gamma \rho_A^2(\gamma) - f_B^2(\gamma) + \pi^2 \rho_B^2(\gamma)\right]$$

$$\rho_s(\gamma) = -2\frac{f_B(\gamma)}{d(\gamma)} \left[\gamma \rho_A(\gamma)\, f_A(\gamma) - \rho_B(\gamma)\, f_B(\gamma)\right] + \frac{\rho_B(\gamma)}{d(\gamma)} \left[\gamma\, f_A^2(\gamma) - \pi^2 \gamma \rho_A^2(\gamma) - f_B^2(\gamma) + \pi^2 \rho_B^2(\gamma)\right]$$

Phenomenological Model

Duarte, Frederico, WP, Ydrefors PRD 105, 114055 (2022)

We can calibrate the model to reproduce Lattice Data for $M(p^2)$

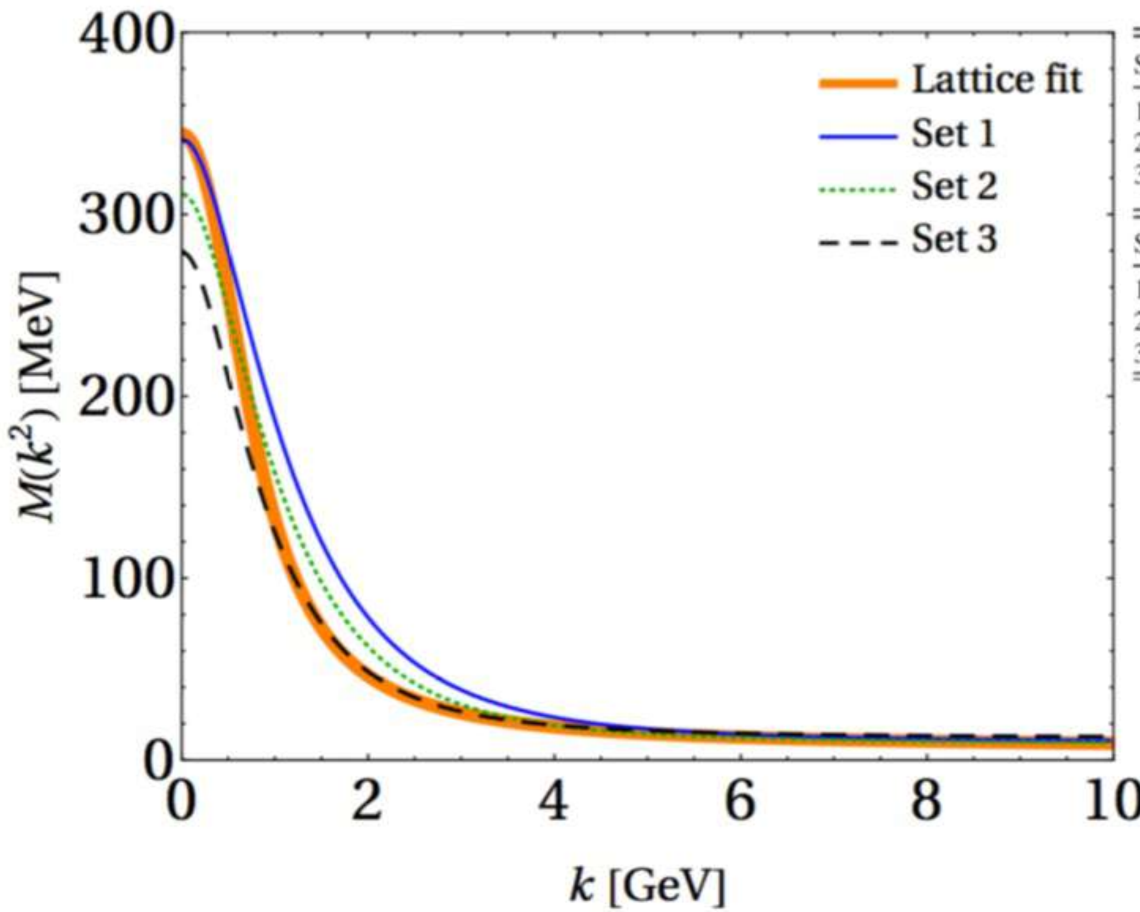

Set	$\bar{m}_0$ (GeV)	m_g (GeV)	Λ (GeV)	α
1	0.42	0.84	1.20	19.70
2	0.38	0.78	1.10	20.30
3	0.35	0.60	1.00	13.25

Set	(Outputs)	m_B (MeV)	R
1		9.06	2.22
2		8.53	2.09
3		12.25	2.64

Lattice data from: Oliveira, Silva, Skullerud and Sternbec, PRD 99 (2019) 094506

IN PROGRESS

- ✓ **BSE in Minkowski space: Quark self-energies (simple model);**
- ✓ **Quark self-energies: SDE in Minkowski space & chiral symmetry breaking;**
  [D. Duarte et al PRD105, 114055 (2022)]
- ✓ **Pion FF and T-even TMDs;**

FUTURE

- ➢ **T-odd TMDs, GTMDs (DGLAP&ERBL)**
- ➢ **Fragmentation Functions**
- ➢ **Dressed Quarks & Gluons, different gauges**
- ➢ **Confinement & quark-gluon vertex**
- ➢ **kaon, D, B, rho…, and the nucleon,**

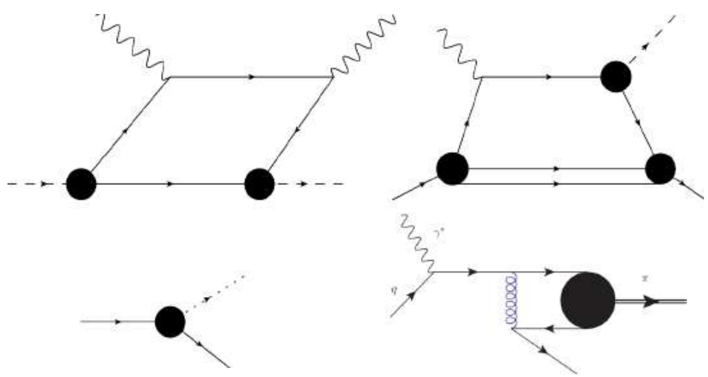

Light-Cone 2023: Hadrons and Symmetries

https://indico.in2p3.fr/event/29047/

18 – 22 de set. de 2023
Rio de Janeiro, Brazil
Fuso horário America/Sao_Paulo

Digite o seu termo de pesquisc

Contact

lightcone2023@gmail.com

The Light-Cone 2023 (LC2023) will be hosted by the Brazilian Center for Physics Research - CBPF from September 18 to 22, 2023 in the city of Rio de Janeiro, Brazil.

Registration will be open by May 1 to August 31, 2023.

The Brazilian Center for Physics Research (CBPF) is one of the most important institutions in Brazil, where both theoretical and experimental research are developed, offers an ideal and stimulating environment to achieve the goals of the conference, thanks to their active community acting in many aspects of the Standard model and beyond.

The conference continues a series that started in 1991 and, since then, takes place at least once a year under the supervision of the **International Light Cone Advisory Committee.**

The scientific goal of the Light Cone conference series is to continuously update the knowledge in light-front theory, its intersections with Euclidean Lattice and continuum approaches towards the phenomenological applications to describe hadrons and nuclei. Light-front theory provides a suitable framework for the calculations of decay rates, scattering amplitudes, correlations, spin effects, phases, distributions and other

THANK YOU!

THANKS TO

CAPES CNPq FAPESP INCT-FNA

IRP/CNRS - SUBATOMIC PHYSICS: FROM THEORY TO APPLICATIONS

CAPES/COFECUB project

Backup slides

Schematic view: TMDs & PDFs

FSI gluon exchange: T-odd

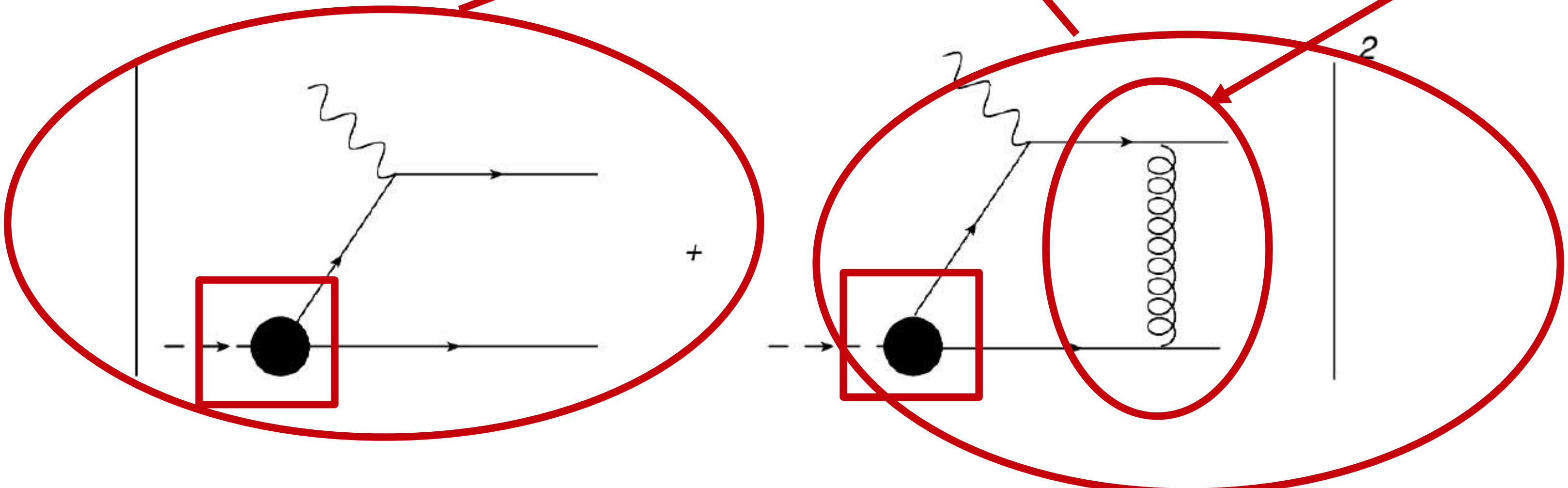

TF & Miller PRD 50 (1994)210

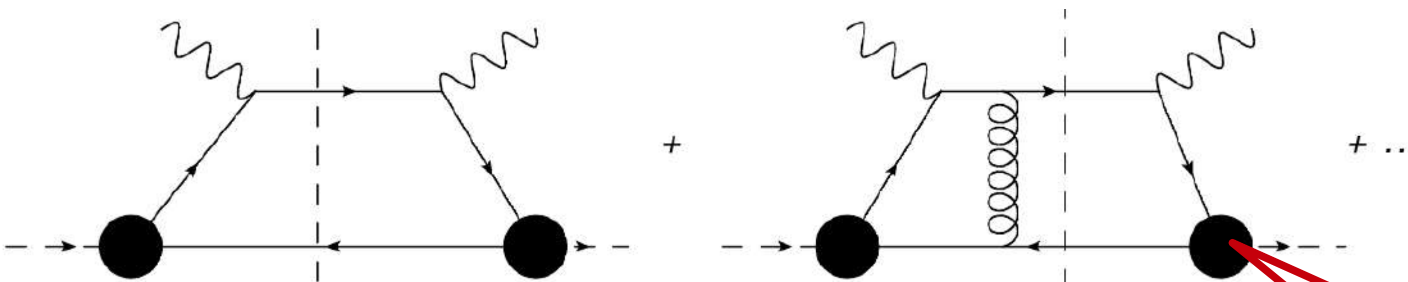

$q^- \longrightarrow$ *infty*
DIS

Bethe-Salpeter Amplitude @ $x^+=0$

$$q^2 = q^+q^- - q^2_T$$

$$q^+ = q^0+q^3 \quad q^- = q^0-q^3$$

Generalized Stietjes transform and the LF valence wave function

Carbonell, TF, Karmanov PLB769 (2017) 418 (bosons)

$$\boxed{\Psi_i(\gamma, z; \kappa^2) = \int_0^\infty d\gamma' \frac{g_i(\gamma', z; \kappa^2)}{[\gamma + \gamma' + m^2 z^2 + (1 - z^2)\kappa^2]^2}}$$

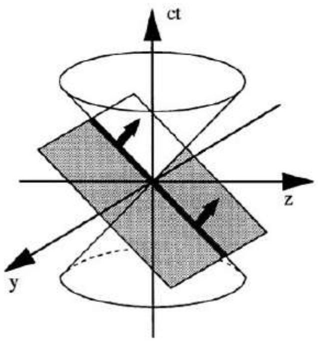

$$\gamma = k_\perp^2 \qquad z = 2x - 1$$

BS amplittude

valence wf

$$\begin{tikzcd}
\chi \arrow[rr, "\text{LF projection}"] & & \Psi_2 \arrow[dl, "\text{Inverse Stieltjes transform}"] \\
& g \arrow[ul, "\text{NIR}"] &
\end{tikzcd}$$

J.H. Schwarz, J. Math. Phys. 46 (2005) 014501,

UNIQUENESS OF THE NAKANISHI REPRESENTATION

PHENOMENOLOGICAL APPLICATIONS from the valence wf → BSA!

Generalized Stietjes transform and the LF valence wave function II

Carbonell, TF, Karmanov PLB769 (2017) 418

$$f(\gamma) \equiv \int_0^\infty d\gamma' \, L(\gamma,\gamma') g(\gamma') = \int_0^\infty d\gamma' \, \frac{g(\gamma')}{(\gamma'+\gamma+b)^2}$$

denoted symbolically as $f = \hat{L}\, g$.

$$g(\gamma) = \hat{L}^{-1} f = \frac{\gamma}{2\pi} \int_{-\pi}^{\pi} d\phi \; e^{i\phi} \; f(\gamma\, e^{i\phi} - b).$$

J.H. Schwarz, J. Math. Phys. 46 (2005) 014501,

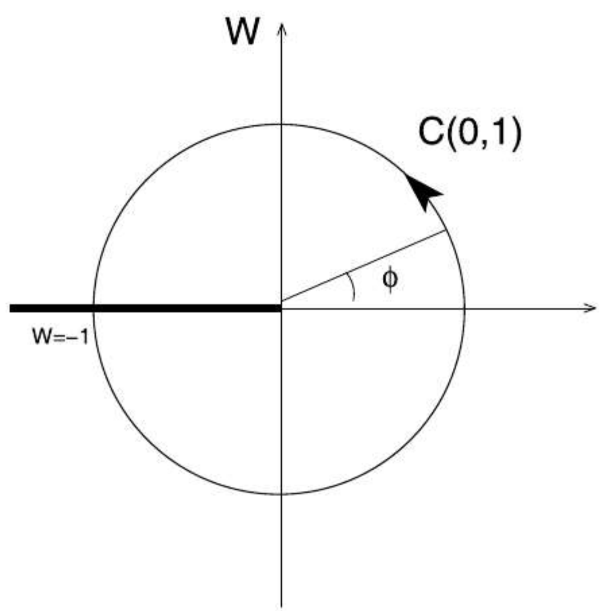

- Kernel of the LF projected pion BSE with NIR
- end-point singularities in the k^- integration (zero-modes)

T.M. Yan , Phys. Rev. **D 7**, 1780 (1973)

$$\mathcal{I}(\beta, y) = \int_{-\infty}^{\infty} \frac{dx}{\left[\beta x - y \mp i\epsilon\right]^2} = \pm \frac{2\pi i\ \delta(\beta)}{\left[-y \mp i\epsilon\right]}$$

→ Kernel with delta and its derivative!

End-point singularities– more intuitive: can be treated by the pole-dislocation method
de Melo et al. NPA631 (1998) 574C, PLB708 (2012) 87

Light-front amplitudes

B/m	M_π (MeV)	g^2	μ (MeV)	Λ/m	m (MeV)	p_{val}
1.35	140	26.718	430	1.0	215	0.68

Kernel has similar magnitude with LQCD form-factor ~ 50%

ψ_1

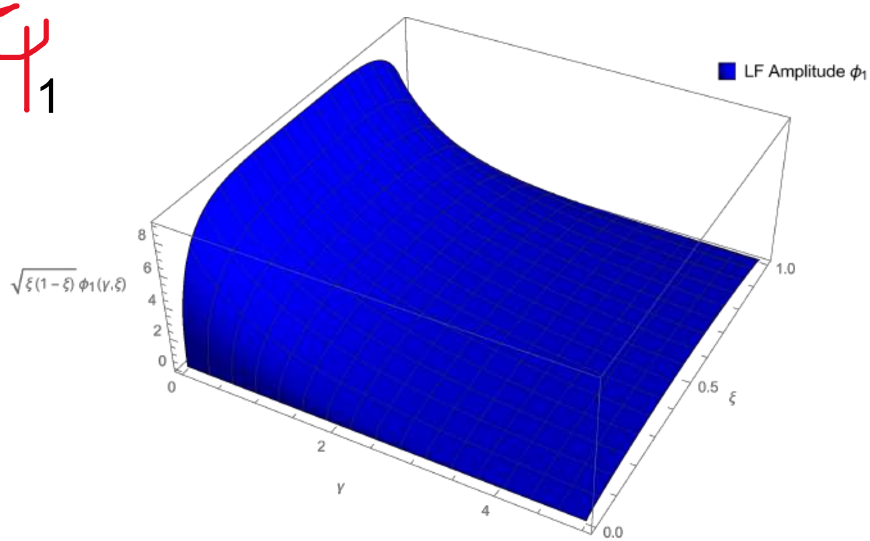

ψ_2

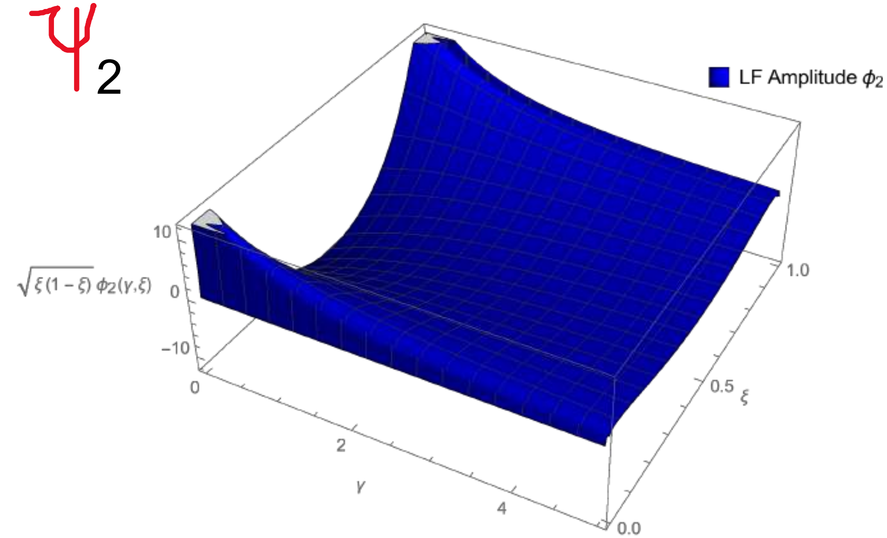

ψ_3

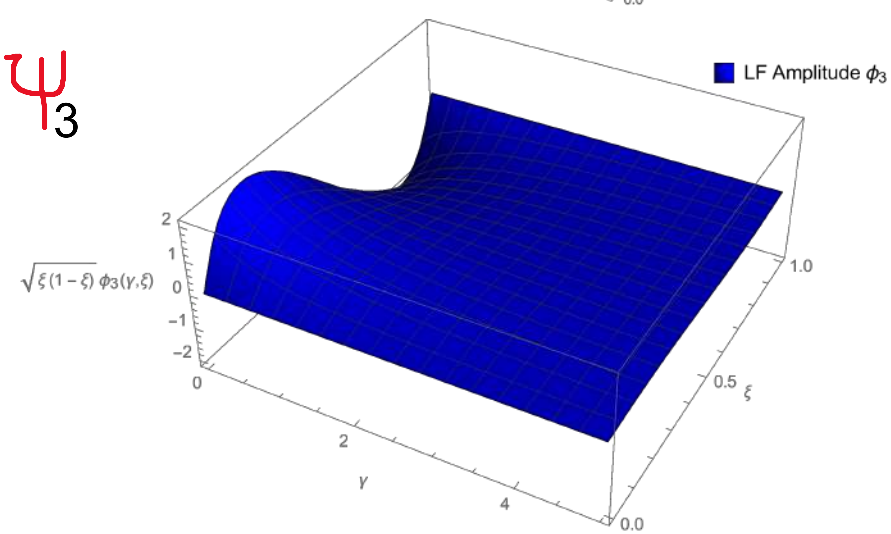

ψ_4

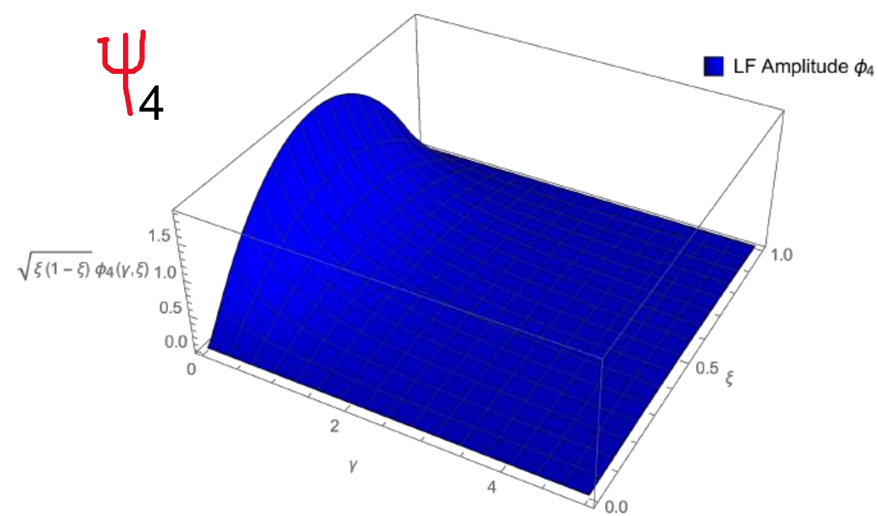

Valence form factor

$$F_{\text{val}}(Q^2) = \frac{N_c}{16\pi^3}\int d^2k_\perp \int_{-1}^{1} dz\left[\psi^*_{\uparrow\downarrow}(\gamma',z)\psi_{\uparrow\downarrow}(\gamma'',z) + \frac{\vec{k}'_\perp\cdot\vec{k}''_\perp}{k'_\perp k''_\perp}\psi^*_{\uparrow\uparrow}(\gamma',z)\psi_{\uparrow\uparrow}(\gamma'',z)\right]$$

$$\vec{k}'_\perp = \vec{k}_\perp + \frac{1}{4}(1-z)\vec{q}_\perp, \quad \vec{k}''_\perp = \vec{k}_\perp - \frac{1}{4}(1-z)\vec{q}_\perp = \vec{k}'_\perp - \frac{1}{2}(1-z)\vec{q}_\perp$$

Asymp. form factor
$$F_{\text{val}}(Q^2)|_{Q^2\to\infty} \sim \frac{N_c}{16\pi^2}\int_{-1}^{1} dz\,\psi_{\uparrow\downarrow}\left(\frac{(1-z)^2}{4}Q^2, z\right)\int_0^\infty d\gamma\,\psi_{\uparrow\downarrow}(\gamma,z)$$

$$F(Q^2) = \int_{-1}^{1} dz \tilde{F}(Q^2,z)$$

Valence pion GPD

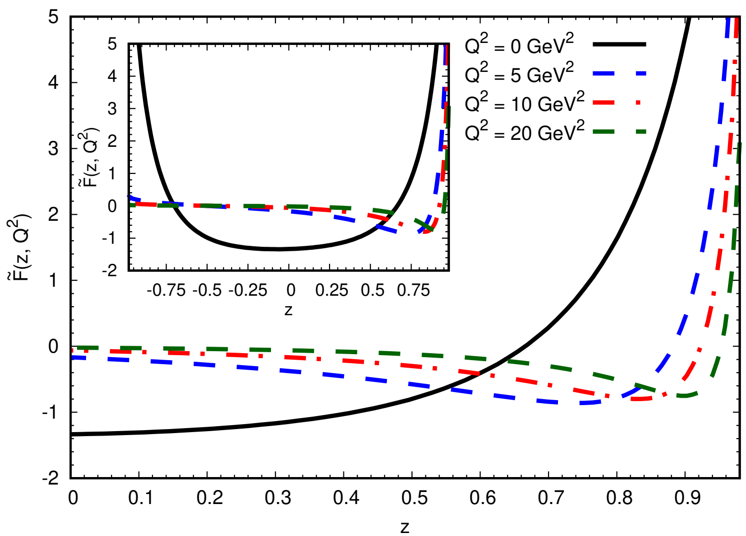

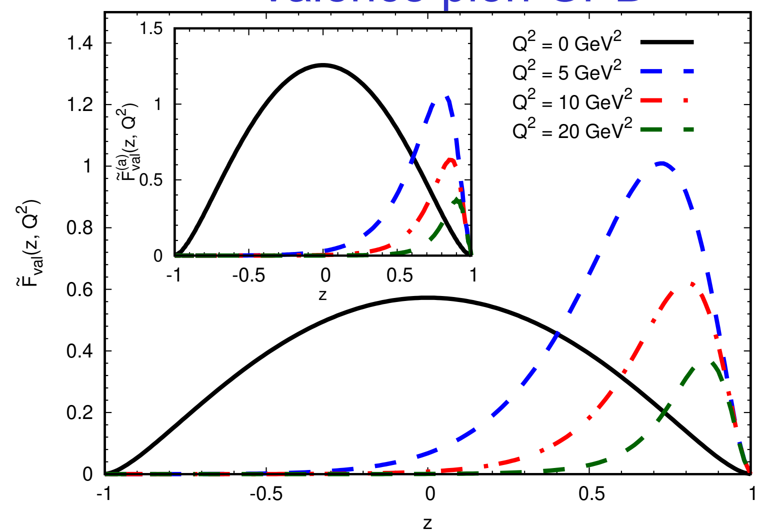

Figure 4: Left: Integrand of the full form factor vs z for fixed values of Q^2. In the main frame are shown the results for $z \geqslant 0$ and in the inset the results for the full interval are visible. Right: The corresponding results for the valence form factor. In the main frame the results obtained by using the complete formula are shown. In the inset the results for the asymptotic formula are displayed. For the visibility the results for $Q^2 > 0$ have been multiplied by a factor of 10.

EVOLUTION

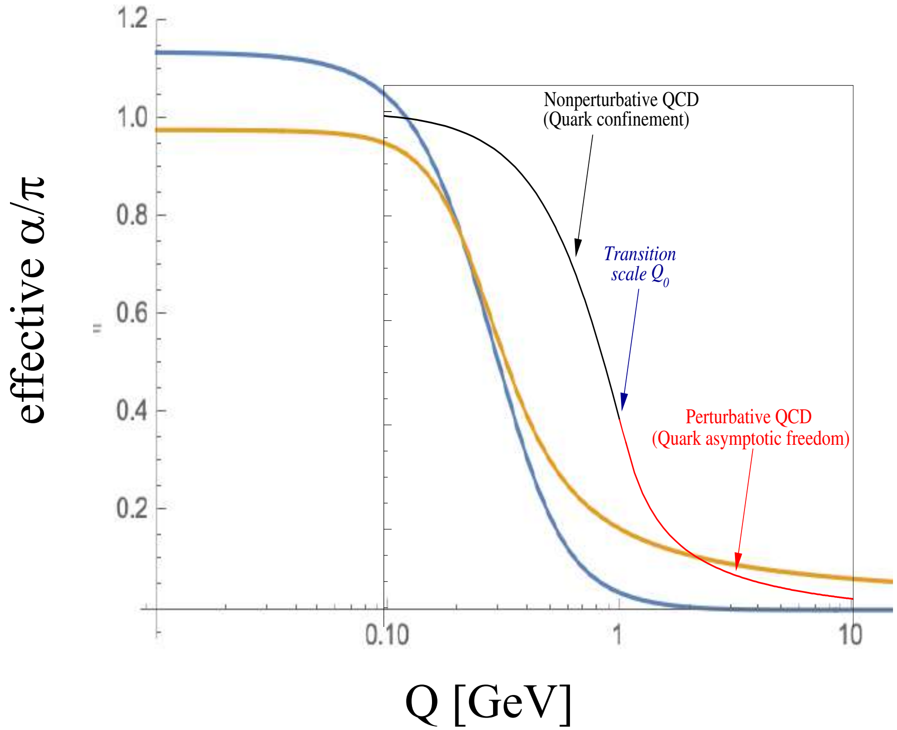

[5] Z. F. Cui, M. Ding, J. M. Morgado, K. Raya, D. Binosi, L. Chang, J. Papavassiliou, C. D. Roberts, J. Rodríguez-Quintero, and S. M. Schmidt, Concerning pion parton distributions, Eur. Phys. J. A **58**, 10 (2022), arXiv:2112.09210 [hep-ph].

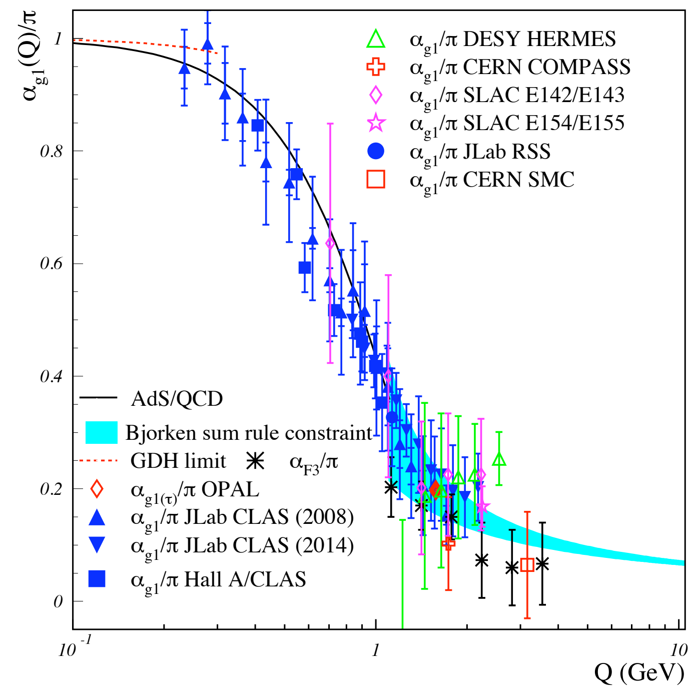

[6] A. Deur, S. J. Brodsky, and G. F. de Teramond, The QCD Running Coupling, Nucl. Phys. **90**, 1 (2016), arXiv:1604.08082 [hep-ph].

LO evolution with effective α

ECLO = Effective Coupling Leading Order Evolution

$$Q_0 = 0.330 \pm 0.030 \text{ GeV}$$